PETROLOGY AND GEOCHEMISTRY OF SOME IGNEOUS INTRUSIVES IN THE

BACK RIVER VOLCANIC COMPLEX, DISTRICT OF MacKENZIE,

NORTHWEST TERRITORIES

PETROLOGY AND GEOCHEMISTRY OF SOME IGNEOUS INTRUSIVES IN THE

BACK RIVER VOLCANIC COMPLEX, DISTRICT OF MacKENZIE,

NORTHWEST TERRITORIES

By

D. LOUISE BEAUMONT

Submitted to the Department of Geology

in Partial Fulfilment of the Requirements

for the Degree

Honours Bachelor of Science

McMaster University

April, 1978.

BACHELOR OF SCIENCE (1978)   McMaster University
(Geology)   Hamilton, Ontario

TITLE: PETROLOGY AND GEOCHEMISTRY OF SOME IGNEOUS INTRUSIVES IN THE

    BACK RIVER VOLCANIC COMPLEX, DISTRICT OF MacKENZIE, NORTHWEST

    TERRITORIES

AUTHOR: D. Louise Beaumont

SUPERVISOR: Dr. P.M. Clifford

NUMBER OF PAGES: vii, 61

SCOPE AND CONTENTS:

   Granitic intrusives and a zoned gabbroic dyke situated within
the Back River Volcanic Complex were mapped and studied. Petrography
and geochemical analyses were performed on selected specimens. Chemi-
can variation diagrams suggest that the granites may have been derived
from the fractional crystallization of a single parent magma. In order
of decreasing age, these granitic units are defined as follows:

  1. Hornblende Quartz Syenite

  2. Granite

  3. Quartz Monzodiorite

   A zoned gabbro/quartz gabbro dyke cuts the granites. Pyroxene
and plagioclase are the dominant minerals of this dyke, and are found
to vary antipathetically throughout the central portions of the dyke.
Chemical studies of this system suggest that the zoning may be the
result of a series of multiple injections from different source magmas.

TABLE OF CONTENTS

LIST OF TABLES

LIST OF FIGURES

CHAPTER I

INTRODUCTION

(1) Location and Accessibility

The Back River Volcanic Complex (Figure 1) is found centred at approximately 65°N, 108°W, in the Slave Structural Province of the Canadian PreCambrian Shield, and covers an area approximately 58 kilometers N-S by 44 kilometers E-W. The mapped area is located on the border between sheets numbered 76 C/16 and 76 B/13 of the National Topographic Series, and can also be found to straddle the 1:250,000 76C Alymer Lake and 76B Healey Lake Topographic map sheets.

The area of intrusives mapped by the author (Figure 1) is located at 64°45'N, 108°00'W and is situated within the Back River Volcanic Complex. It is roughly circular in shape, and approximately 700 meters in diameter.

This remote area, accessible only by float-equipped aircraft, is located about 485 kilometers (300 miles) northeast of Yellowknife, N.W.T.

(2) Previous Work

Regional mapping programmes in the past have reconnoitered the Back River Volcanic Belt. Barnes and Lord (1954), Fraser (1964), Wright (1967), and Tremblay (1971) have each been responsible for this in part.

In 1975, a more detailed mapping project was initiated by the Geological Survey of Canada, to map the Back River Volcanic Belt at 1:25,000 scale. This work was carried out under the leadership of Dr. M.B. Lambert, and was completed in the summer of 1977. Preliminary reports on this work have been published (Lambert, 1976, 1977, 1978).

(3) Statement of the Problem

In June of 1977, while employed by the Geological Survey of Canada, the author undertook the mapping of a small area of intrusives within the Back River Volcanic Complex. Initial interest was generated due to the unusual, almost round shape of the intrusives, and the great length of the MacKenzie Type dyke which also cuts them.

This area has not previously received more than reconnaisance mapping. Although similar types of intrusives were observed throughout the Complex during its recent detailed mapping, nowhere else were they found in such a unique configuration as that observed here.

The goal of this project was to produce a detailed map (2.5 cm to 30.0 meters) of the intrusives and surrounding volcanics, showing the distribution of seven rock units found within, their contact relationships and structural features, as well as a discussion of their petrological and chemical characteristics.

During the course of mapping, one hundred and eleven samples were taken, thirty-five of which were prepared for thin section study, and thirteen of which were studied by means of chemical analysis. The map in the back pocket of book indicates sample localities.

(4) Preparation for Field Work

In order to map effectively such a small area on a very detailed scale, it was necessary to lay out a grid over the area, prior to the commencement of mapping. This was accomplished by placing marker cairns at 30 or 60 meter intervals from a central point of origin. Mapping was then plotted on grided paper.

(5) Acknowledgements

I am grateful to Dr. M.B. Lambert, of the Geological Survey of Canada, who originally suggested this topic, and who allowed collection of field data during the 1977 field season. His advice during the actual mapping, as well as throughout its writing have proved invaluable, and is sincerely appreciated. I would also like to thank the other members of the field party: Mr. R.M. Easton, Mr. J.A. Percival, and Mr. J.P. Sorbara for help in collecting data, useful discussions, and encouragement.

My supervisor, Dr. P.M. Clifford, provided excellent guidance and advice throughout, whose help was also deeply appreciated.

Chemical analyses were performed by the Geological Survey of Canada and Mr. Otto Mudroch. Thin section preparation was performed by the Geological Survey of Canada and Mr. Len Zwicker. Mr. Jack Whorwood provided assistance with photography. Many of the professors and undergraduates of McMaster University gave helpful suggestions. Thanks must go to all of these people.

The fine work of Mrs. Jan Gallo in typing the manuscript is also appreciated.

Figure 1

4

Regan Lake

−65°   65°

Contwoyto River

Back River

Magrum
Lake

108°

0   km   5

Coronation
Gulf

■ map

Gt. Slave
Lake

– – –Limit of Back River Volcanic Complex

■   Area Mapped in Detail
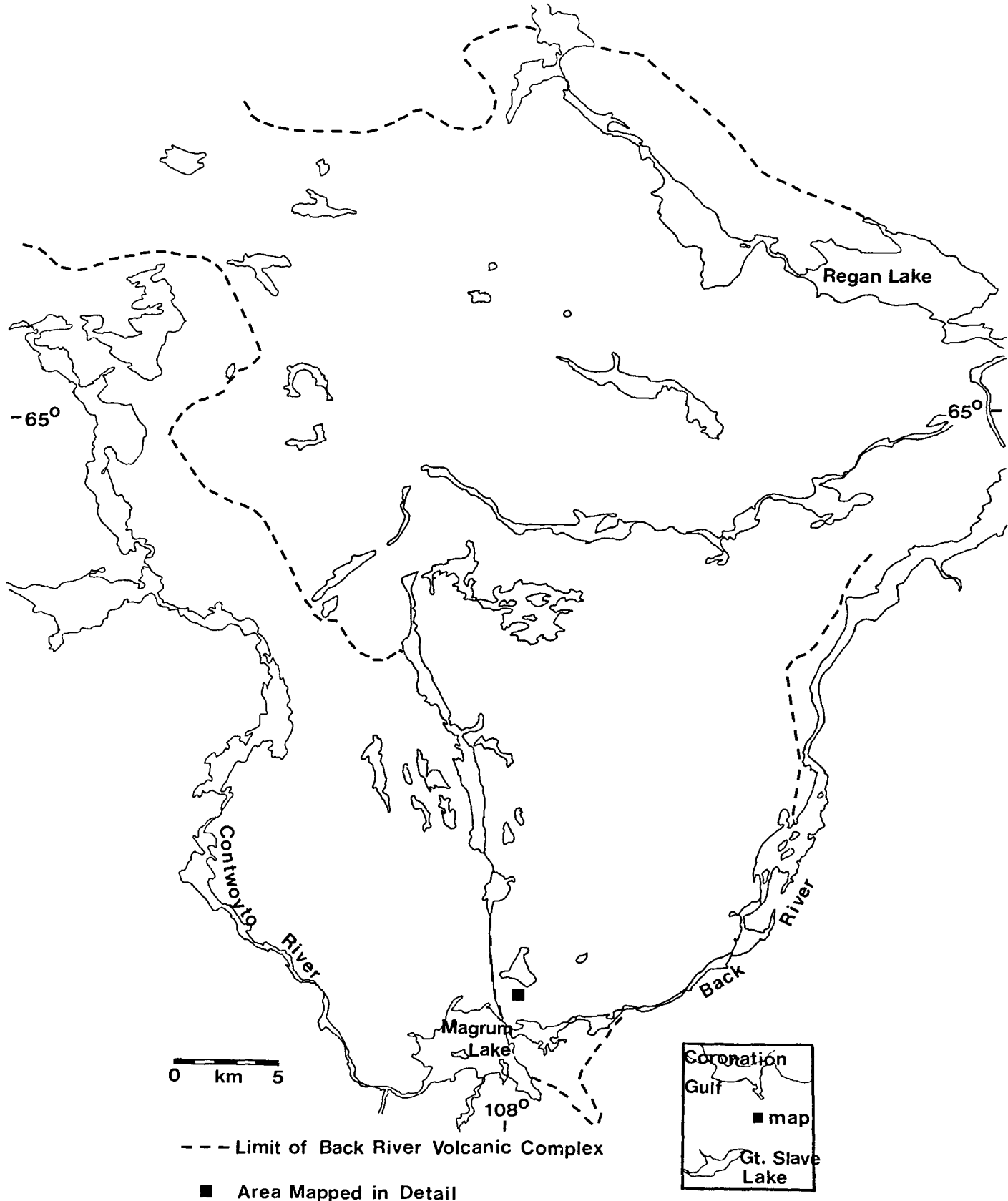
after Lambert (1978)

CHAPTER II

GENERAL GEOLOGY

(1) Yellowknife Supergroup

The term "Yellowknife Supergroup" (Henderson, 1970) has been applied to both volcanic and sedimentary rock units of Archean age, throughout most of the Slave Province. The volcanics and sediments of the Back River Volcanic Province are seen to be representative of Yellowknife Supergroup rocks (Lambert, 1977).

Within the Yellowknife Supergroup (Douglas, 1970), volcanic sequences from 300 to 12,000 meters thick are composed largely of basic volcanic flows. These may take the form of massive, pillowed, or variolitic flows, in which occur banded tuffaceous layers. Flows, tuffs, and breccias of intermediate to acid composition are generally rather scarce in this Supergroup, but tend to be common in the upper portions of the thicker sequences. Chemically (Douglas, 1970), the basic volcanics are tholeiitic basalts with calc-alkaline characteristics. The volcanics are commonly intruded by sills, dykes, and irregular-shaped bodies of massive, fine grained diorites or gabbros, which are chemically equivalent to the flows. And finally, the igneous rocks are overlain by thick sedimentary sequences of quartz-rich greywackes, or feldspathic greywackes, interbedded with argillites and shales.

(2) Back River Volcanic Complex

The Back River Volcanic Complex forms one of the largest areas

of felsic volcanic rocks in the Slave Province (Henderson, 1975). It
consists of felsic to intermediate volcanics, including tuffs, breccias,
and lavas, as well as minor amounts of basalt (Lambert, 1977). The
basalts are generally found to be pillowed and brecciated, while the
andesites are usually plagioclase-porphyritic massive flows and tuffs,
the dacites massive, and the rhyolites quartz-porphyritic. The volcanic
tuffs and breccias are most commonly andesitic to dacitic in composition.
The volcanics conformably overlie Archean aged greywackes and mudstones
of the Yellowknife Supergroup (Henderson, 1970). Both volcanics and
sediments are cut by gabbro dyke swarms and granodioritic to adamellitic
plutons (Lambert, 1977). Many of the dykes in the Back River Volcanic
Complex are of the Mackenzie Type. These are diabasic in composition,
vertical-dipping, northwest-trending, and have been dated at about 1200 M
years (Douglas, 1970). Other related swarms found in this area trend
East, yielding Potassium-Argon ages of 2150 M years, or Northeast, giving
ages of 2100 M years, and are of comparable composition (Douglas, 1970).
The generation and relation between the gabbroic dykes and granitic
plutonic rocks are of primary interest in this project.

(3) General Setting of the Mapped Area

The mapped area (see map located in back flap of book), located
near the southwest margin of the Back River Volcanic Complex, measures
approximately 700 meters N-S, by 730 meters E-W. Mapping has defined
two units of volcanic rocks, three coarse grained, often hornblende-
porphyritic units of igneous intrusives, and a zoned gabbro-monzonite
dyke. The volcanic flows and tuffs found here are representative of

those found throughout the entire Back River Volcanic Complex (Lambert, 1978), and can be subdivided into recrystallized tuffaceous andesites and dacites, and quartz-porphyritic rhyolite flows. The three granitic intrusive phases collectively tend to form a roughly semi-circular out-crop pattern, which wraps around a central tuffaceous core, opens to the north, and is in turn largely surrounded by rhyolites. And finally, there is a northwest-trending gabbro-quartz gabbro Mackenzie Type dyke, which extends for several kilometers through the complex. This dyke forms a major and prominent feature in the western portion of the Back River Volcanic Complex, and in the mapped area in particular.

CHAPTER III

PETROGRAPHY

A number of hand specimens and thin sections have been selected
for study from each unit mapped. The map in back flap of book shows the
locations of these specimens in relation to the field area.

All specimens have been named using the IUGS classification
scheme (Geotimes, October, 1973), applied to the results of modal analysis.
Approximately 1000 to 1500 points were counted per slide to give these
analyses. Figure 2 plots the results in terms of the components quartz,
alkali feldspar, and plagioclase. Figure 3 shows quartz plotted against
total feldspar and total mafics, complements the three previous figures,
and gives a relative colour index. Figure 4 shows the relative amounts
of pyroxene and amphibole in the modal analyses, thus giving some indica-
tion of relative amounts of secondary alteration. In cases where the
specimen was too fine grained to obtain accurate modal analyses, the
rock name was obtained from the results of chemical analyses.

(1) Gabbroic Dyke Rocks

In hand specimen, these rocks tend to weather a light to dark
pinkish-grey colour. This distinctive colour, plus the fact that the
outcrops weather to a very hard, rounded surface, makes dyke rocks fairly
easy to distinguish from the other intrusives in the area. The gabbro
is a uniform, medium grained, equigranular rock, which usually shows a

pink weathering rind approximately 1-2 mm deep on all weathered surfaces.
Quartz and feldspar crystals are left relatively unaffected by weathering,
and stand in high relief relative to the mafic minerals, which are generally
deeply eroded. These medium to coarse grained rocks appear to be composed
of about 60% mafics and 40% felsics. Minor feldspar alteration can be
noted as a pink colouration around many of the crystals, or occasionally
as a greenish tinge. Plagioclase crystals are visible on the fresh sur-
face in hand specimen, grown in various relations to the mafic crystals.
They can be seen to be intergrown with the mafic minerals (77B8LQ1),
to form rims around the mafics as in 77B52LQ1, or to occur as discrete
laths of up to 2 mm length, as in sample 77B50LQ1. Mafic grains in the
gabbros range from about 3 to 5 mm length.

In this section, the gabbros are relatively constant in their com-
positional and textural relations. The mineral phases clinopyroxene,
amphibole, plagioclase, quartz, and opaque oxide are present in similar
quantities in each specimen. Clinopyroxene is probably augitic in com-
position, occurring as subhedral prismatic phenocrysts, often with in-
clusions parallel to the cleavage traces. Amphibole phenocrysts (probably
Hornblende) are euhedral, containing very small opaque inclusions around
which the cleavage traces kink.

Plagioclase, which makes up 50-60% of the gabbro samples studied,
is the single most abundant constituent. It tends to occur in euhedral
laths, which are usually quite long relative to the other crystals.
Most of these crystals are severely altered, so that they appear cloudy
and indistinct in form. The alteration takes the form of microcrystalline

fibrous aggregates of muscovite and sericite, and is most prominent along the direction of the twin planes. The composition, as determined from Michel-Lévy tests performed on many plagioclase laths, ranges from An_{36} to An_{66}. Quartz occurs as small, anhedral interstitial grains, which contain very small, unrecognizable angular inclusions.

Opaque oxides are the major accessory minerals, found evenly distributed through the rock. These occur as anhedral to subhedral crystals, some of which approximate square or six-sided forms, which may possibly be pyrite or magnetite. Opaques commonly form inclusions in the augite, but are never found associated with plagioclase. Other minor constituents are alkali feldspar, in the form of microcline, and kinked biotite.

Texturally, the gabbros are holocrystalline and hypidiomorphic granular. Large amounts of felsic material in the gabbros occur in the form of spectacular myrmekitic intergrowths (Figure 5), which form much of the sample, in which some of the quartz exhibits good undulose extinction. Pyroxenes tend to be interstitially located between plagioclase laths, thus forming a sub-ophitic texture (Figures 6 and 7). Pyroxenes may also form long, highly birefringent stringers, lying between adjacent parallel aligned plagioclase laths. The opaque minerals are often closely associated with the pyroxenes; one mineral frequently enveloping the other. This elongated crystal form often is observed in the oxides as well. A sharp chilled contact is developed where the dyke lies adjacent to other rock units. The contact against quartz monzodiorite is shown in hand specimen in Figure 8 and in thin section in Figure 9.

(2) Quartz Gabbro Dyke Rocks

In hand specimen, the weathered surface of these more felsic dyke rocks is very similar in colour and texture to the gabbroic rocks discussed above. The rocks in this unit are medium grained and equi-granular, containing mafic crystals of up to 2 to 3 mm length, alkali feldspars approximately 2 to 3 mm length, plagioclase 1 mm, and scattered quartz crystals of 2 mm length.

In thin section, the dominant mineral phase is plagioclase, which occurs in very large laths, and constitutes 60-65% of the rock. Plagio-clase appears cloudy due to extreme alteration to muscovite and sericite. This alteration concentrates along the original twin planes to such an extent that they are now obscure, or have been obliterated completely. Amphibole phenocrysts form roughly 10-20% of the rock as a whole, and are dominantly large, dark brown to green, euhedral crystals, which rarely display any cleavage. Opaque oxides forming approximately 5% of the rock, are found as relatively large, anhedral crystals, approximately the same size as the amphiboles. Quartz and feldspar occur in large crystals of myrmekite.

These larger phenocrysts lie surrounded by numerous much smaller crystals of quartz, amphibole, biotite, opaques, and minor pyroxene. Chlorite and epidote occur in this unit as accessory minerals in the groundmass. Textures shown in Figure 10.

(3) Quartz Monzodiorite

The Quartz Monzodiorite outcrop is very massive. A distinct zone of alteration from a fresh grey to a bright pink altered rock runs in a

strip approximately thirty meters wide, roughly parallel to the strike of the dyke. The zone is especially noticeable to the east of the dyke. The rocks display slightly increasing grain size and decreasing alteration with distance from the dyke. A weathering rind approximately 2 mm thick develops on all weathered surfaces. Its colour may range from cream to bright pink, depending on proximity to the dyke. On the whole, the quartz monzodiorites are equigranular, with most crystals 2 to 3 mm in length. The felsics tend to be more anhedral in shape, while the mafics are usually platey.

In thin section (Figure 11) plagioclase laths, moderately altered to sericite and muscovite, and still showing some relict twinning, make up about half of the section. From Michel-Lévy tests performed on the twin planes, composition has been determined to be labradorite, of approximately An_{54}. A green biotite is the only mafic mineral, making up 15-20% of the rock. It occurs as small, fibrous, plate-like intergrowths of crystals, in interstitial clumps, distinctly segregated from the other minerals in the section. Small biotite laths are often found lined up tangentially around the margin of much larger quartz crystals.

The quartzo-feldspathic groundmass of the quartz monzodiorites consists of large areas of clustered alkali feldspars, plagioclase feldspars, and quartz, lying between bands of aligned biotite flakes. This alignment is evident only on a microscopic scale. The quartz crystals in the groundmass are virtually undeformed, and there is a clustering of the smaller crystals around the larger quartz or plagioclase crystals. Extremely small amounts of opaque oxide (much less than 1% of the rock)

occur as small crystals nested in the biotite areas of the rock, but are never seen associated with the felsics. Chlorite and minor epidote are accessory minerals.

(4) Granite

These intrusives occur in three separate regions of the mapped area. From the mineralogy and modal analyses performed on samples from each area, it is obvious that, although they are not identical in physical appearance, all three areas probably represent portions of the same intrusive phase.

In hand specimen, all unaltered rocks from these granitic intrusives have a dark coloured, fine grained groundmass. However, the colour is highly variable, dependent on the degree of alteration imposed by proximity to the dyke. It is pinker and more altered closer to the dyke, where elsewhere it weathers to a grey to black mottled colour. The most prominent feature of these intrusives is the mafic phenocrysts. Specimens one or two meters from the dyke have small euhedral phenocrysts, ranging from the microscopic, up to about 3 mm length. The size of the euhedral phenocrysts changes to become larger with distance from the dyke. Forty meters west of the dyke, the phenocrysts are in the order of 7 mm length, and are lath-shaped, no longer perfectly euhedral. At 45 meters, where the intrusion lies against the rhyolites, hornblendes are found up to 10 mm in length, along with biotite flakes up to 7 mm length. This very coarse margin to the intrusion is peculiar in that it is composed solely of large crystals, including biotite, pyroxene, amphibole and alkali feldspar (Figure 12). Its mineralogy is somewhat different from

the rest of the intrusion, yet is very similar to another coarse grained area, associated with the margin of the eastern outcrop of this unit.

Thin sections of these granitic intrusives are all very much alike, with the exception of the changing size and degree of alteration of the phenocrysts. These consist of largely unaltered, well-cleaved augitic pyroxene crystal cores, which in most cases, have been variably altered to tremolite-actinolite amphibole around the periphery. Most of the smaller pyroxene crystals are subhedral; the larger ones are euhedral (Figure 13). The alteration to amphibole from pyroxene in these crystals appears to proceed from the outside to the centre. In one specimen (77B42LQ1) from the northeast corner of the mapped area, where the pyroxenes are largely unaltered, they tend to be clustered, intergrown, and twinned instead (Figure 14). It is in this same area that the pyroxene phenocrysts are found to be nucleated around anhedral, fragmental opaque oxides; a relationship not seen elsewhere.

Biotite laths also occur as phenocrysts in the rocks of this unit, but are consistently smaller in size than the pyroxene or amphibole crystals. Biotite always occurs as a minor mineral phase, and in several cases may be found associated with the pyroxene crystals, often forming interstitial masses between the larger phenocrysts.

The felsic groundmass comprises approximately half of the bulk of these intrusives. It is composed of intergrown crystals of quartz, plagioclase, and alkali feldspar, whose fine grain size does not allow the accurate distinction of individual components in thin section. It contains small muscovite laths as well, which are considered to be part of the felsic groundmass. Only in the very coarse grained margin of this

unit do we find exception to these observations. Here there is no "ground-mass" as observed previously, but instead the felsic component consists of coarse grained, coherent crystals of microcline and sanidine, with no quartz, plagioclase, or muscovite present.

Opaque oxides, calcite, and chlorite form the accessory minerals.

(5) Hornblende Quartz Syenite

In hand specimen, this unit weathers a light pink to white colour, with 5-6 mm black weathering, subhedral to euhedral mafic phenocrysts. The phenocrysts are randomly oriented, and appear black around the edges, but green in the centres. Colouration may imply secondary alteration here. A weathering rind about 1 cm thick develops around all exposed surfaces, showing a colour change from a greyish pink to a pinkish white. On the fresh surface can be seen the fine grained pink felsic groundmass, in which lies the dense aggregation of euhedral mafic phenocrysts.

In thin section, this unit appears very similar to the granite intrusives discussed above in terms of modes and mineralogy. Pyroxene phenocrysts are the most striking feature of this unit; they are large subhedral to euhedral crystals which have been selectively altered to amphibole around their edges. The smaller the crystal, the more completely altered it will be. The pyroxene crystals are often seen to be twinned. The twin plane sometimes divides the crystal such that one-half remains as unaltered pyroxene, while the other half is completely altered to amphibole. This unit was named on the basis of its present composition, not its primary composition.

The feldspathic groundmass is still the major constituent of these intrusives, occupying roughly half their volume. It is made up of many small, interlocking crystals of untwinned feldspars, plus considerable amounts of microcline, and minor quartz. Large areas of the groundmass have been altered to a cloudy beige coloured material, adjacent to the alteration rims of the pyroxenes.

Accessory quantities of opaque oxides occur as small subhedral to euhedral grains, not normally found associated with any specific mineral phase. Instead, they occur as inclusions in the pyroxene, amphibole, biotite, and groundmass. Biotite also forms a minor phase in these intrusives, as does chlorite.

(6) Rhyolite Volcanics

In hand specimen, the Rhyolites weather to a characteristic creamy, polished, marble-like surface, with a distinctive subconchoidal fracture, which almost gives the appearance of being bone. A chalky white weathering rind forms to a depth of approximately 1.5 cm on all exposed outcrop surfaces. The fresh surface of the Rhyolites can range in colour from white to pink to translucent brown or grey. The white and pink varieties represent altered outcrop, while grey fresh surfaces are indicative of unaltered rock. Quartz phenocrysts 1-2 mm diameter are set in an aphanitic groundmass.

In thin section, relatively large, anhedral, unstrained quartz phenocrysts, devoid of inclusions, are a very prominent feature, and are set in a felsic groundmass (Figure 15). Smaller, evenly-distributed, euhedral opaque mineral grains also occur as phenocrysts in this unit,

around which small mafic crystals tend to cluster. This opaque phase
is probably Magnetite or Ilmenite.

These rocks are so very fine grained that even in thin section,
the minerals of the groundmass are almost indistinguishable. However,
it can be determined that the groundmass consists of quartz and untwinned
plagioclase feldspar, plus very small green, sparsely-distributed,
lath-like mafics, which are probably biotite.

(7) Tholeiitic Andesite Tuff

This unit consists of clasts which weather differently from the
surrounding groundmass in which they are situated. The clasts weather
grey, brown, or green, and are best observed on lichen-free exposures,
or freshly broken surfaces. Fresh surfaces show a dark grey or green
aphanitic matrix, in which are embedded slightly lighter coloured frag-
ments. The clasts range in shape from the extremely angular to those
which are markedly inequant, some of which reach 10 cm in length. The
texture appears "welded" (Lambert, personal communication). The clasts
are often inequant in shape, with a fine grained recyrstallized texture,
sitting in an almost aphanitic glassy groundmass. The clasts in the
tuffs are aligned at orientations ranging from 122° to 150° relative to
magnetic north. The outcrops are extensively fractured, with alteration
along the fracture planes, trending roughly 130/85E, roughly the same
direction in which the clasts are oriented.

The fragments are composed of crystals much larger in size than
the groundmass (Figure 16), and appear to represent areas of concentra-
tion of mafic minerals. Most of the mafic crystals are small plate-like

laths, although some are larger. These crystals have distinct straw
yellow to dark green pleochroism, one direction of cleavage well defined
along the long axis of the lath, and an extinction angle of 11-12°, so
are probably hornblende. In general, the laths are oriented with their
long axes parallel to the maximum length of the fragment as a whole. A
few scattered anhedral, red-brown, translucent to opaque hematite grains
occur in the fragments. Minute crystals of quartz and feldspar fill the
interstices between the mafic flakes.

The groundmass of these tuffs is almost aphanitic, and quartzo-
feldspathic in nature. The individual felsic crystals seem to show a
very rough alignment parallel to the direction of clast alignment. The
feldspars in the groundmass are untwinned, but the small quartz crystals
possess undulose extinction. It is hypothesized that the above factors,
as well as the alignment of the groundmass crystals, may be due to heat
and pressure, which produced a welded texture in the clasts (Lambert,
personal communication). The mafic constituent of the groundmass takes
the form of many microscopic laths of a green pleochroic mineral, pro-
bably hornblende, as was observed in the clasts. These plates are also
aligned parallel to clasts (see texture in Figure 17).

In terms of the textures seen in the tuffs, most of the fragments
are of the same general shape. They are roughly ovoid, with one end
extended into a point, while the diametrically opposite end of the clast
is abruptly broken off. Pieces of the clast from the broken end are left
behind in small clumps to form a long "tail" on the fragment. "Eyes"
of the groundmass material are frequently seen completely enclosed by a ring
of mafic laths, all of which lie with their long axes parallel to the long
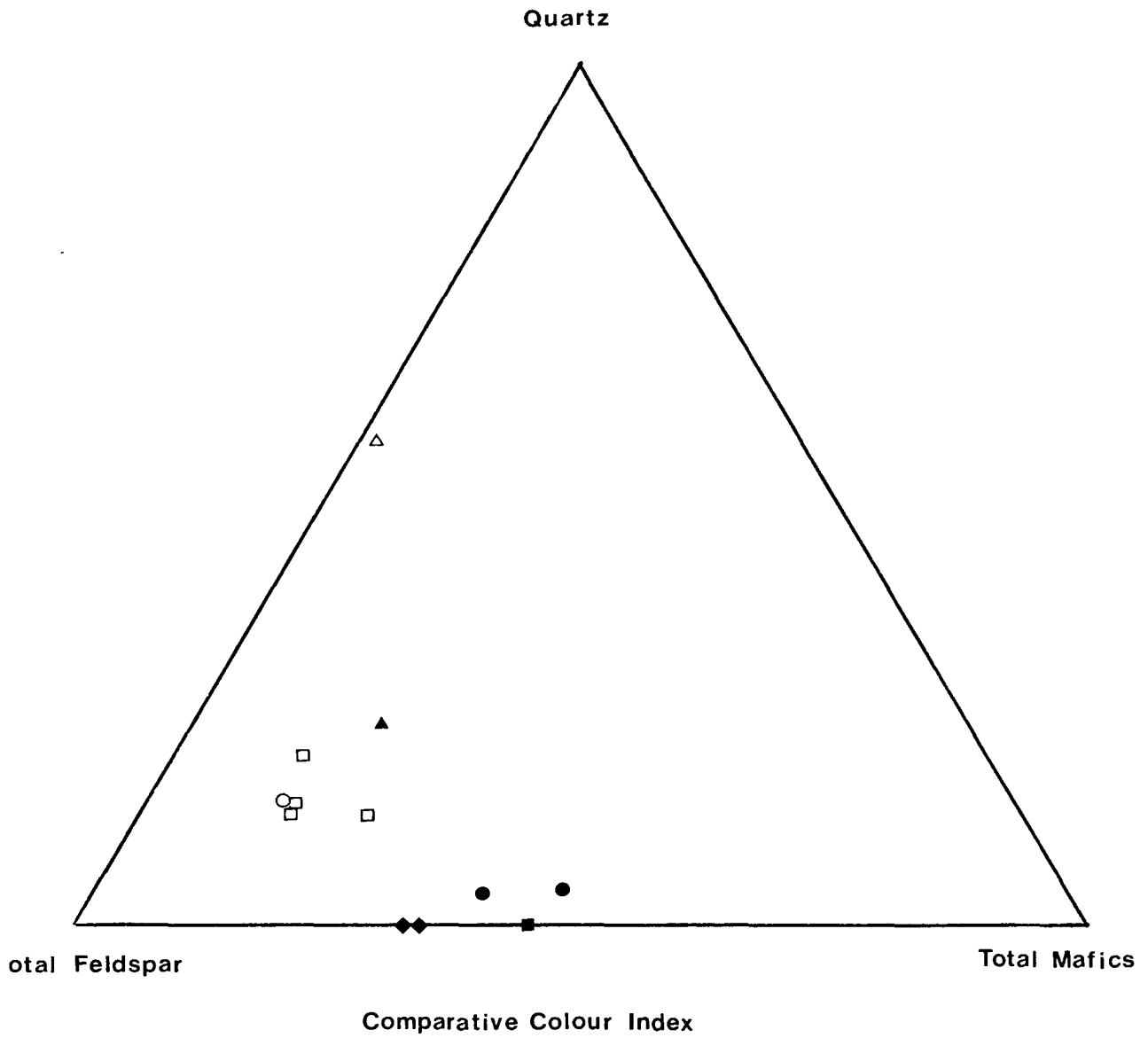direction of the structure.

Figure 2

Plutonic Rock Classification
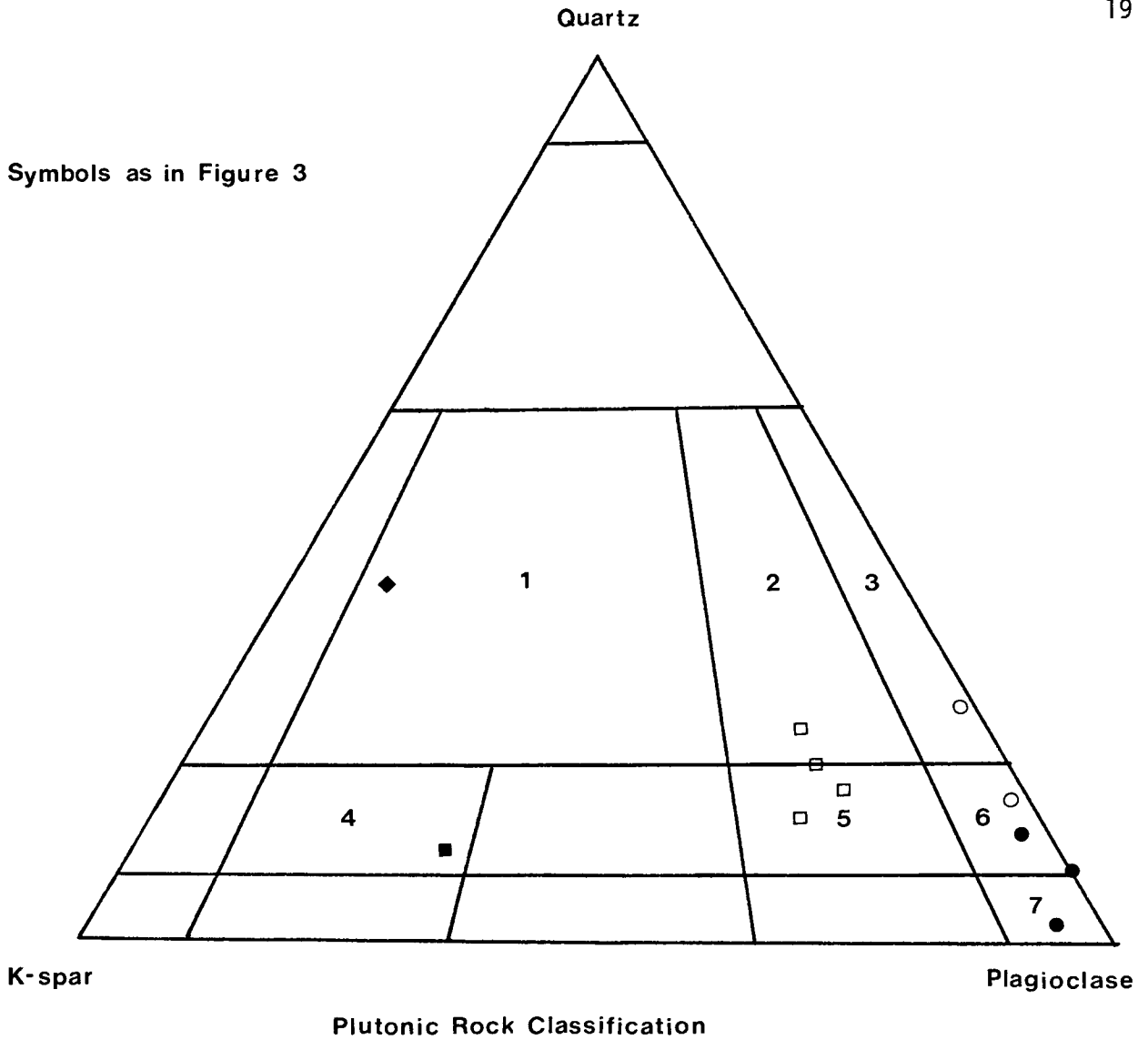
Area No.	Classification
1	Granite
2	Granodiorite
3	Tonalite
4	Quartz Syenite
5	Quartz Monzodiorite
6	Quartz Gabbro
7	Gabbro

Figure 3

Quartz

otal Feldspar

Total Mafics

Comparative Colour Index

▲   Andesite Tuff

△   Rhyolite

□   Quartz Monzodiorite

■   Hornblende Quartz Syenite
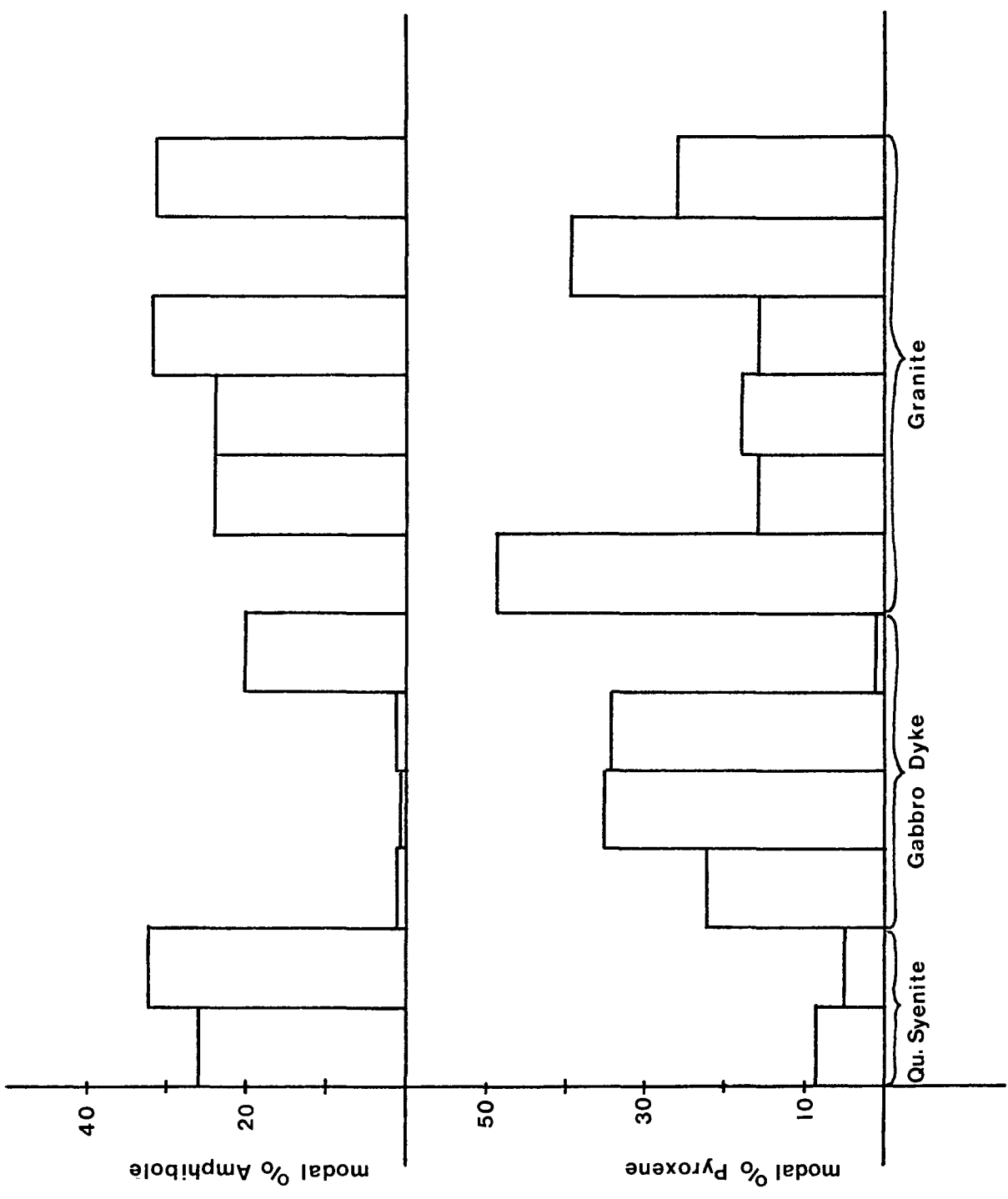
◆   Granite

●   Gabbro

○   Quartz Gabbro

Figure 4

Figure 5

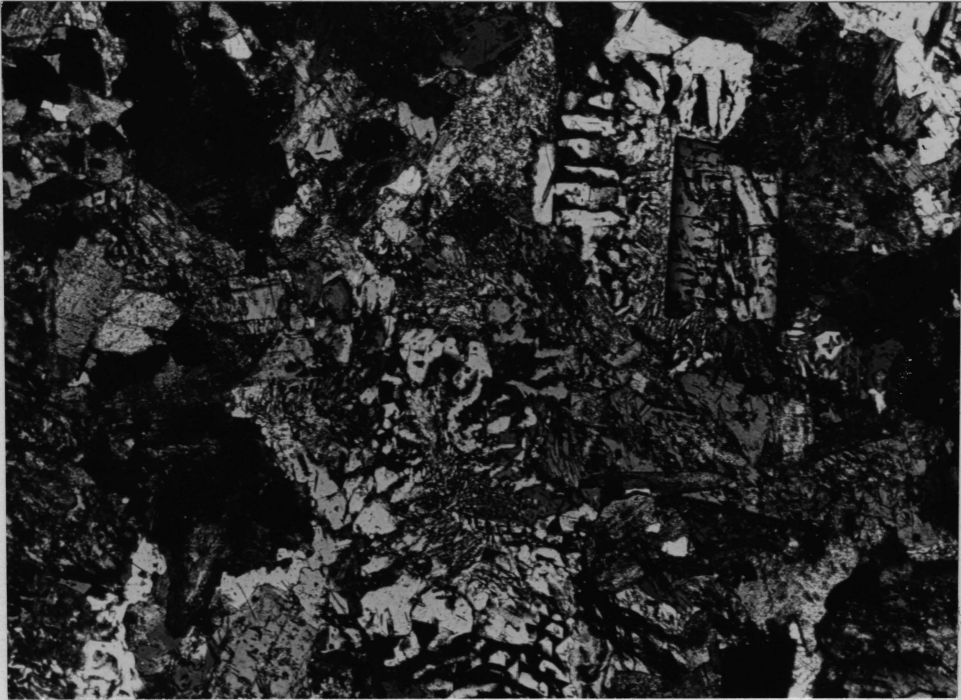Myrmekitic texture developed in a Gabbro

Magnification: 25x

Figure 6

Subophitic texture in a marginal phase Gabbro

Magnification: 25x

Figure 7

Subophitic texture in a Gabbro from the central portion of the dyke

Magnification: 25x

Figure 8

Hand specimen of contact between chilled gabbro dyke (left hand side)

and quartz monzodiorite (right hand side)

Specimen shown is 10 cm wide

Figure 9

Thin section of chilled contact of gabbro dyke showing plagioclase and

pyroxene phenocrysts in very fine grained groundmass

Magnification: 25x
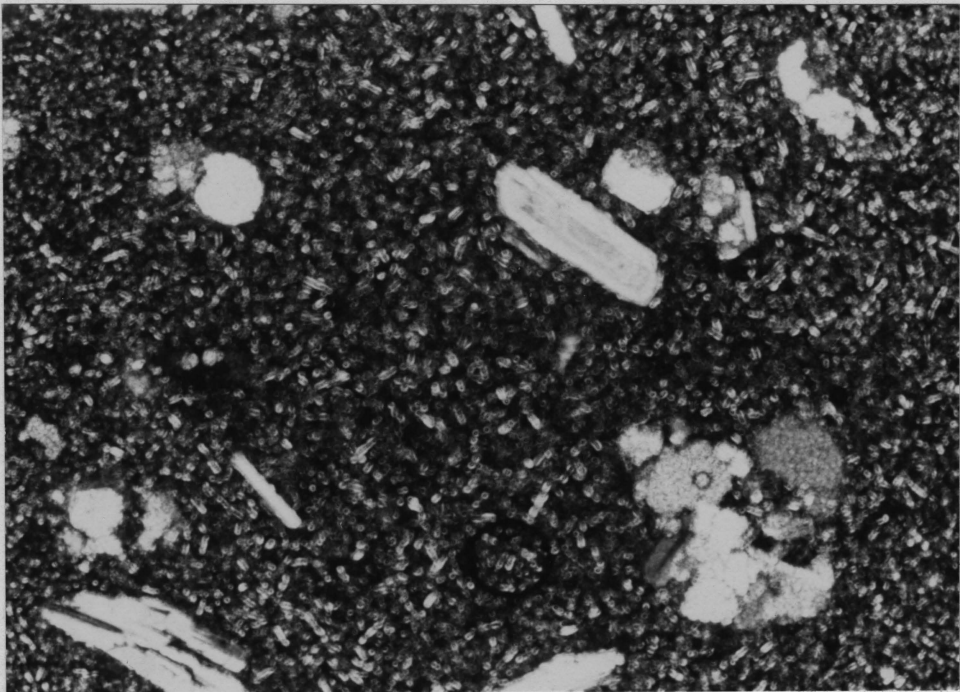
Figure 10

Typical texture observed in Quartz Gabbro, showing areas of myrmekite

Magnification: 25x

Figure 11

Quartz Monzodiorite showing equigranular plagioclase and mafics

Magnification: 25x
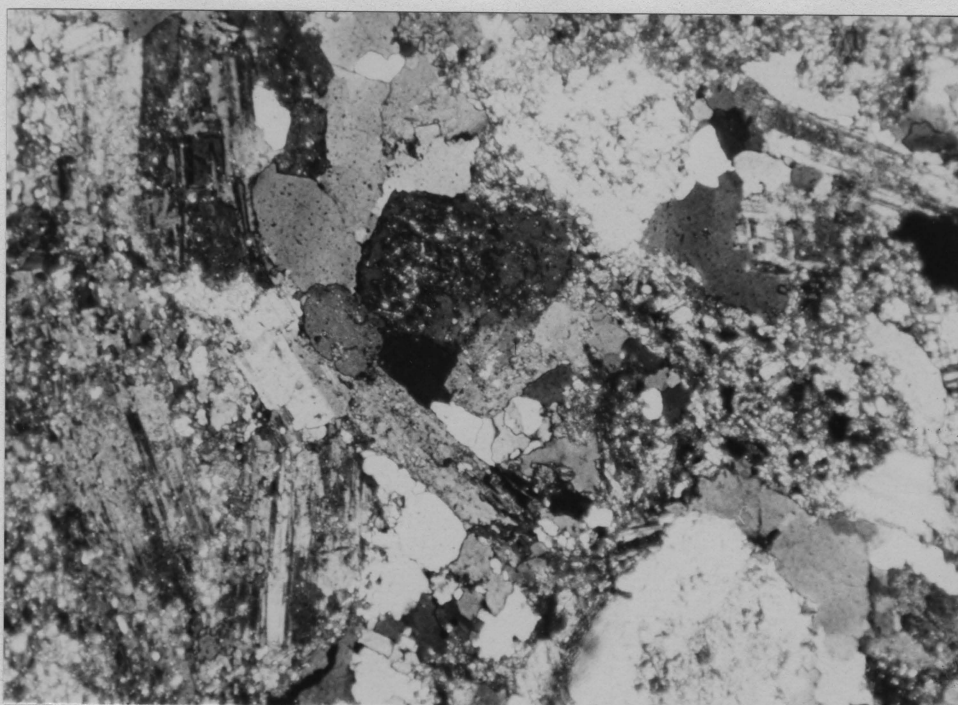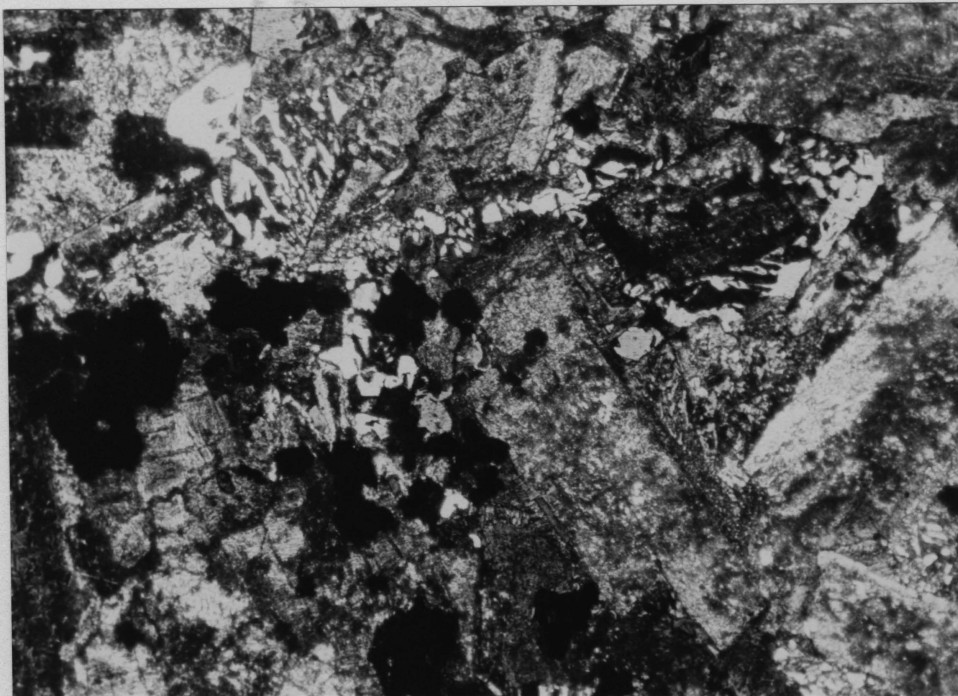
Figure 12

Granite showing large, euhedral pyroxene crystal from coarse grained margin

Magnification: 25x

Figure 13

Twinned and untwinned pyroxene crystals in fine grained granite

Magnification: 25x
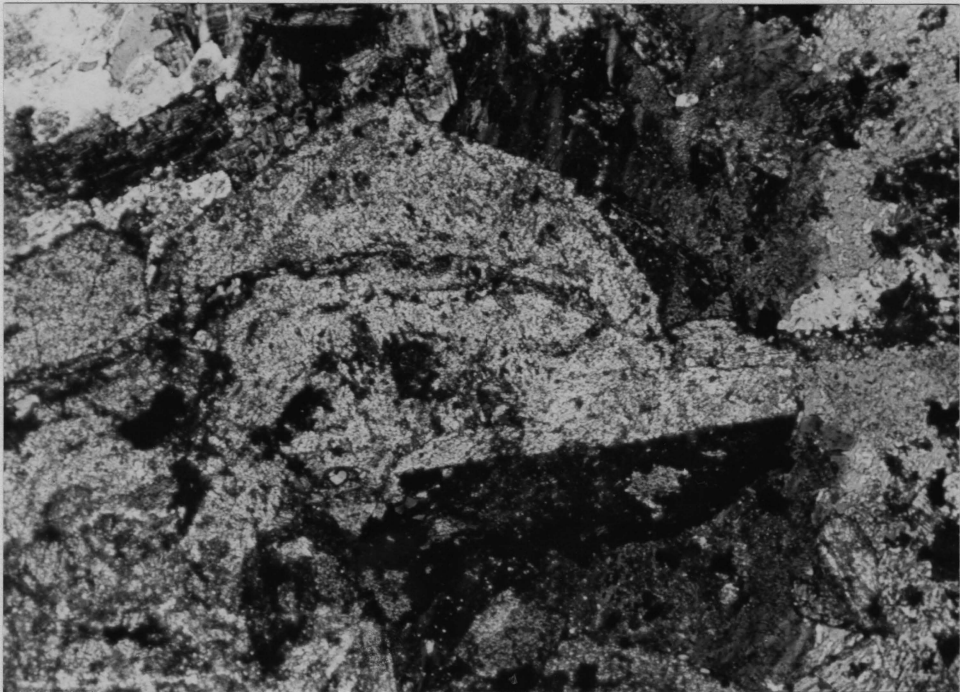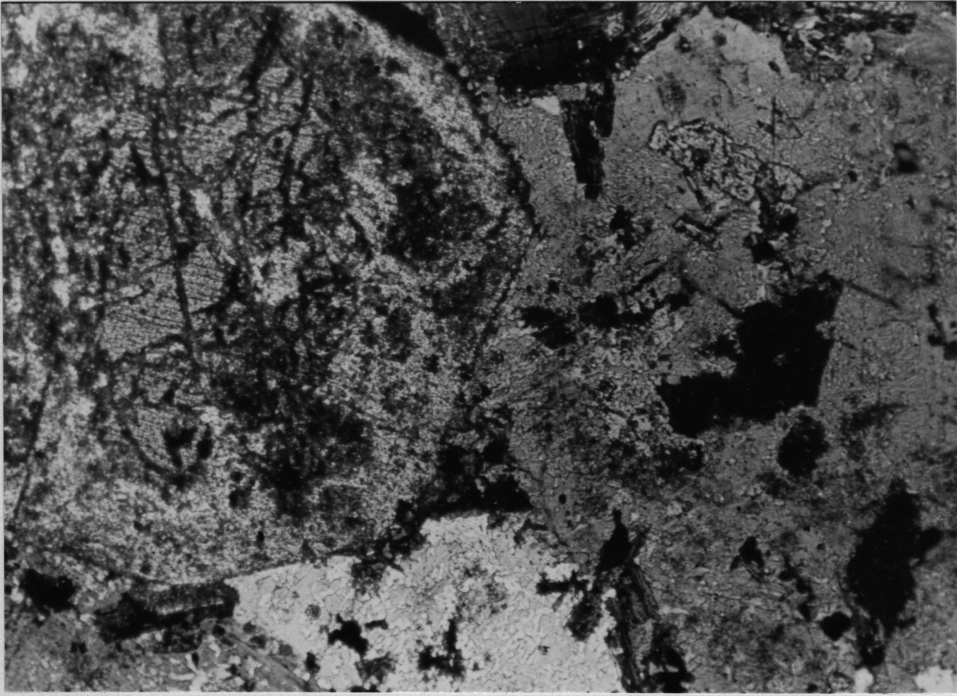
Figure 14

Twinned euhedral pyroxene crystal in Granite

Magnification: 36x

Figure 15

Rhyolite with "Quartz Eye" phenocrysts

Magnification: 25x
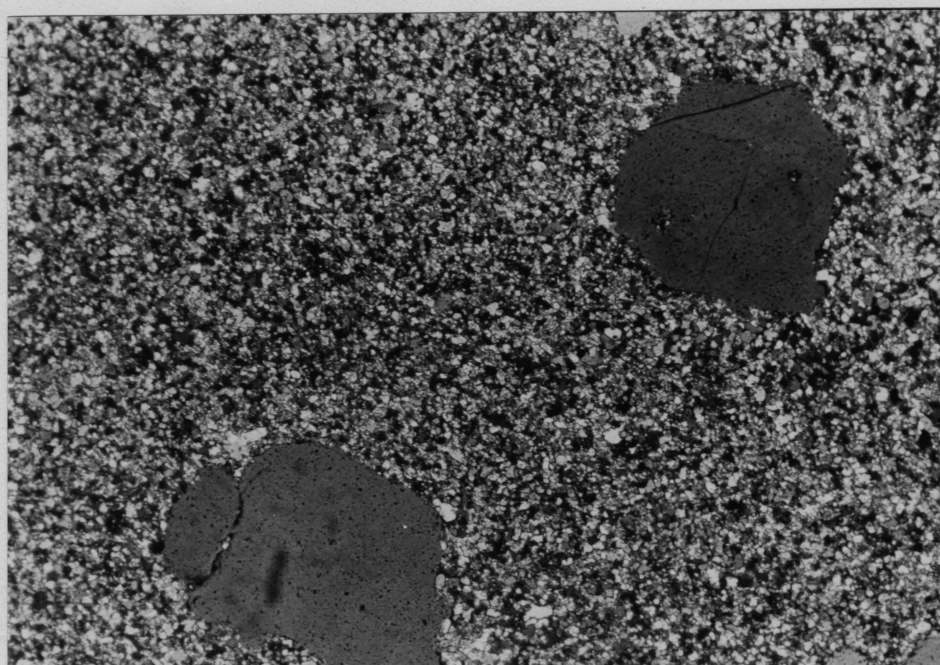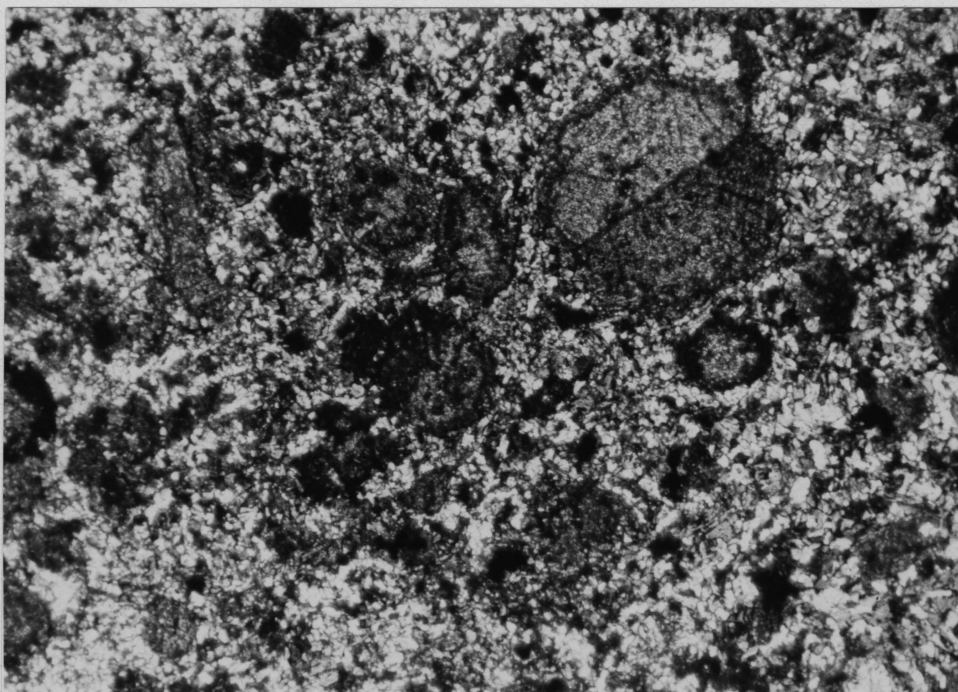
Figure 16

Abruptly terminated tail on fragment in Tholeiitic Andesite Tuff

Magnification: 25x

Figure 17

Rounded nose on fragment in Tholeiitic Andesite Tuff

Magnification: 25x
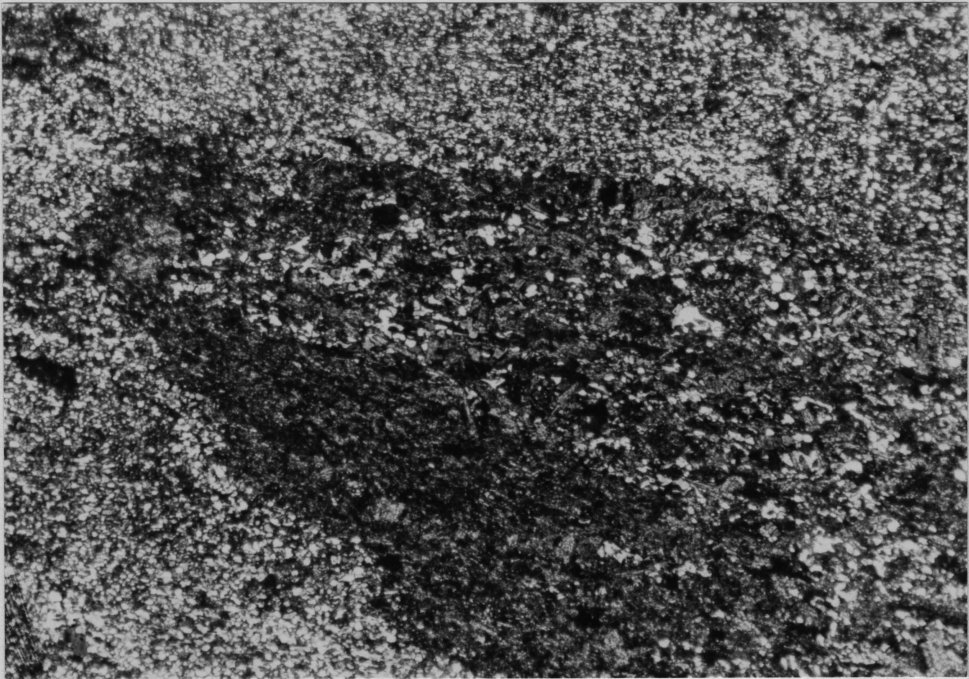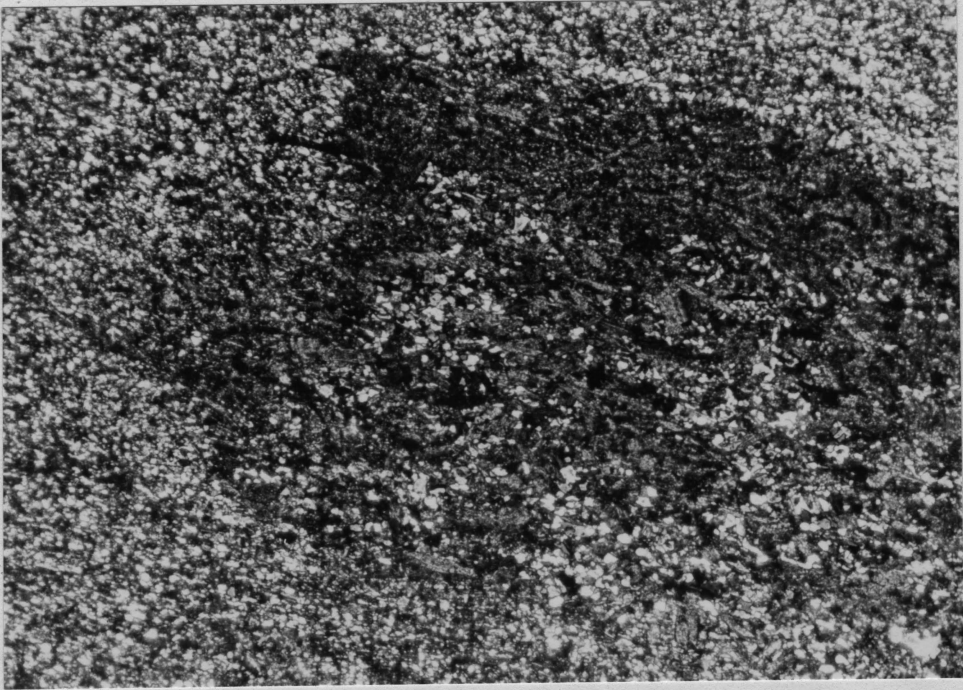
CHAPTER IV

GEOCHEMISTRY

(1) <u>Introduction</u>

Representative samples were taken for chemical studies from each
unit mapped as indicated on map in back flap of book. A total of twelve
samples were analyzed for the author by the Geological Survey of Canada,
and one by Mr. O. Mudroch of McMaster University. Whole rock X-ray
fluorescence analysis was performed to detect the major and minor elements
Si, Al, Fe, Mg, Ca, Na, K, Ti, P, Mn, S, Ni, and Cr as well as CO_2 and
H_2O. Spectrochemical analysis was also applied to detect minor and
trace element abundances such as those of Mg, Ti, Mn, As, Ag, B, Ba, Ce,
Co, Cr, La, Mo, Ni, Pb, Sb, Sn, Sr, V, Y, Yb, Zn, and Zr. Analysis by
X-ray fluorescence is expected to be more precise for those elements
which occur in higher concentrations, while optical emission is more
accurate for lower element concentrations such as are found in trace
element abundances. The data from this work was then analyzed by a
Geological Survey of Canada computer programme, which calculated and
printed information such as weight percents of the oxides, CIPW norms,
norm ratios, differentiation index, and colour index for the rocks.

Weight percentages, CIPW norms and Spectrochemical Results are
outlined for each sample analyzed in Tables I, II and III, respectively.

(2) <u>Chemical Trends</u>

The information obtained from chemical analysis is displayed in

Figures 18 through 21.

The most common method of visualizing such data is to plot the weight percentages of various oxides against a variation index of some sort. Bowen (1928, in Carmichael, Turner, and Verhoogen, 1974) advised against the use of variation diagrams in the interpretation of porphyritic or coarse grained rocks because he believed these rocks not to be representative of a "continuous line of descent" when cooling, thus resulting in considerable scatter about the expected curves.

Although the specimens studied here are generally in good agreement with the anticipated results of this type of plot, it must be kept in mind that the rocks in question are both coarse grained, and porphyritic. This would invalidate these results in Bowen's mind.

Figure 18 plots weight percents of various oxides against the Larsen Index, where L.I. = Weight $\%(\frac{Si}{3} + K - Ca - Mg)$. This particular diagram gives a better fit to the data points than can be obtained by using many of the other variation indices which are currently popular. The general trends shown by the data from this area indicate that SiO_2, K_2O, and Na_2O increase linearly, while MgO and $(FeO + Fe_2O_3)$ decrease along a curved path, and Al_2O_3 shows an increase, followed by a decrease with increasing Larsen Index. These trends are developed in many igneous bodies, and are thought to indicate that either the magma has undergone fractional crystallization, or that all of the rocks plotted originated from the same parent magma (Carmichael, Turner and Verhoogen, 1974).

It is interesting to note that the curve for MgO appears to show what may be separate granitic and gabbroic trends. These two trends eventually merge into one, possibly indicating separate cooling of gabbroic

and granitic magmas to this point.

Associated with both alkali trends are several points which fall extremely far from the expected curves. For the case of the K_2O curves, it can be seen that both the granite and hornblende quartz syenite analyses lie a great distance above the K_2O curve, so are found to be strongly enriched in potash. And with respect to the Na_2O curve, both andesite and rhyolite lie at considerable distances below the curve, thus indicating that the volcanics in this area are strongly depleted in sodium.

Another valuable way of displaying this type of chemical data is by the use of AFM diagrams which plot (K_2O + Na_2O) vs. (FeO + Fe_2O_3) vs. (MgO). Figure 19 shows this information. As can be seen from studying this Figure, the data falls along three distinct trends, which are separate for the dyke rocks, the granites, and the volcanics. Also plotted is the trend for the Palisades Sill and a Calc-Alkaline suite from the Cascade Province.

The results indicate that the volcanics, granites, and quartz gabbro all show calc-alkaline affinities, while the gabbros show a tholeiitic affinity.

Mapping indicates that within the granitic units, the age relations are as follows: Hornblende Quartz Syenite is oldest, the Granite unit is intermediate in age, and the Quartz Monzodiorite unit is youngest. This chronology is verified by the AFM diagram, in that the points within each unit cluster closely, indicating insignificant chemical variability within the unit, while the rocks tend to become more alkaline and less mafic as they lose large amounts of hornblende phenocrysts with decreasing age.

Close comparison between trends shown by the Palisades Sill and the dyke rocks shows that they are very similar in shape. The major difference appears to be that the Palisades trend has been shifted slightly, such that it is enriched in magnesium. Similar arguments can be made for comparison between the Calc-Alkaline Cascades trend and the Granitic trend. The shape of these two curves is virtually identical, except that the Cascades curve is somewhat broader, and sits slightly higher than the Granitic trend, indicating that it is enriched in iron to some extent.

A comparison of other known igneous trends from the literature, such as the Skaergaard (Walker, 1969), Stillwater and Bushveld (Wager and Brown, 1967), and Huzi Province, Japan (Turner and Verhoogen, 1960), does not establish any immediate relationships.

By plotting the Felsic Index ($\frac{Na_2O + K_2O}{Na_2O + K_2O + CaO} \times 100$) against the Mafic Index ($\frac{FeO + Fe_2O_3}{FeO + Fe_2O_3 + MgO} \times 100$), as in Figure 20, it is once again evident that a general trend can be established for each of the gabbros, granites, and volcanics. Displaying the data in this form demonstrates quite well the differentiation and cooling of the dyke rock. This produces a change from the gabbroic edges which are enriched in mafic constituents, to the quartz gabbroic core, which becomes extremely felsic, accompanied by a drastic reduction in mafic constituents as cooling progresses.

In the granite, a trend is evident once again which reinforces field data concerning the relative ages of the various granitic units. These three units plot in the same order as before, i.e., Hornblende Quartz Syenite to Granite to Quartz Monzodiotire. This transition involves

only a slight increase in mafic index, while the felsic index rises sharply. These trends reflect actual physical changes in the rock units, which may in fact be due to fractional crystallization from a single parent magma. Large amounts of mafic material are lost during this differentiation (most notably in the form of hornblende phenocrysts), to the extent that the end product (Quartz Monzodiorite) is essentially composed of quartz and feldspars plus biotite.

The volcanics show a constant mafic index in this Figure, accompanied by a sharp increase in felsic index from andesite to rhyolite. This indicates little change in mafic content, at the same time as the felsic content rises substantially in the rhyolite.

Figure 21 is an ACF diagram for this area. It does not provide significant new information. The rock units cluster as before, but are found concentrated in the corner of iron enrichment, except for the rhyolite, which, being extremely felsic, sits in the alkali corner.

(3) Summary

The results of chemical analyses of thirteen samples from the area under study have been plotted in a variety of arrangements and combinations, the most significant of which have been discussed above. In most cases, three distinct chemical trends may be observed; one for each of the gabbros, granites, and volcanics. The granite trend is helpful in reinforcing field relations which give the relative ages of the three units involved. However, despite the encouraging results of this data, it must be kept in mind that the data displays only the results of thirteen analyses, taken from seven different rock units. Therefore, the conclusions reached here may in fact not be an accurate analysis of this configuration of rocks as a whole.

TABLE I Whole Rock Analyses in Weight Percent Oxides

	SiO_2	Al_2O_3	Fe_2O_3	FeO	MgO	CaO	Na_2O	K_2O	TiO_2	MnO	P_2O_5	CO	Total
B42-1	54.60	14.47	2.44	6.32	5.66	6.92	3.26	4.33	0.92	0.14	0.73	0.20	99.99
B43-1	65.38	15.83	1.23	2.67	2.48	3.07	4.63	3.64	0.49	0.06	0.41	0.10	99.99
B44-1	63.86	15.61	0.91	2.84	2.57	3.94	4.76	3.01	0.47	0.07	0.44	1.52	100.00
B45-1	60.61	14.43	1.44	5.88	2.48	6.91	2.47	2.12	1.02	0.19	0.38	2.06	99.99
B46-1	53.55	13.85	2.49	6.60	6.03	7.21	3.08	5.07	0.95	0.15	0.91	0.10	99.99
B47-1	82.75	10.65	0.10	0.31	0.16	0.16	1.64	4.14	0.06	--	0.02	--	99.99
B48-1	65.72	15.20	1.03	2.57	2.47	3.50	4.62	2.67	0.43	0.06	0.39	1.33	99.99
B49-1	63.81	15.09	0.91	3.14	2.53	3.79	4.66	3.49	0.51	0.07	0.48	1.52	100.00
B50-1	48.35	12.35	2.67	14.71	4.63	8.44	2.26	0.93	4.63	0.24	0.79	--	100.00
B51-1	67.39	14.86	1.44	2.06	2.73	2.34	5.16	2.95	0.45	0.06	0.43	0.10	99.97
B52-1	49.46	13.73	3.10	12.70	3.41	7.82	2.89	1.36	4.44	0.20	0.77	0.10	99.98
B53-1	52.48	12.03	2.87	7.31	7.58	8.87	2.28	3.69	1.32	0.21	1.04	0.31	99.99
B33-1	47.58	11.75	5.0	11.16	5.29	9.19	2.17	0.66	3.50	0.24	0.36	--	96.9

TABLE II   In Weight %s (Norms)

Sample No.	Qu	Cor	Or	Ab	An	Di	He	En	Fs	Fo	Fa	Mt	Il	Ap	Ct
7B42LQ1	---	--	25.48	27.44	11.98	7.64	5.61	5.05	4.25	2.67	2.47	3.53	1.73	1.69	0.46
7B43LQ1	14.26	--	21.47	39.03	11.65	0.11	0.08	5.24	4.27	--	--	1.78	0.94	0.95	0.23
7B44LQ1	15.94	1.91	17.77	40.22	7.08	---	--	5.69	4.74	--	--	1.32	0.88	1.01	3.45
7B45LQ1	22.47	1.19	12.52	20.87	18.68	---	--	5.25	9.44	--	--	2.09	1.93	0.88	4.68
7B46LQ1	---	--	29.82	24.44	8.95	9.59	6.90	--	---	6.17	5.61	3.60	1.80	2.11	0.23
7B47LQ1	56.65	3.22	24.47	13.86	0.68	---	--	0.34	0.47	--	--	0.15	0.12	0.05	--
7B48LQ1	20.64	2.36	15.76	39.01	6.36	---	--	5.41	4.24	--	--	1.49	0.82	0.90	3.03
7B49LQ1	14.93	1.41	20.62	39.33	6.06	---	--	5.59	5.22	--	--	1.32	0.96	1.10	3.45
7B50LQ1	4.28	--	5.43	18.99	20.62	4.36	9.05	6.77	16.12	--	--	3.85	8.72	1.82	--
7B51LQ1	17.53	0.20	17.40	43.52	8.11	---	--	5.76	3.30	--	--	2.09	0.86	1.00	0.23
7B52LQ1	4.49	--	8.00	24.28	20.32	3.11	7.58	4.58	12.78	--	--	4.46	8.37	1.78	0.23
7B53LQ1	---	--	21.69	19.17	11.59	11.70	7.47	9.87	7.22	0.88	0.71	4.14	2.48	2.39	0.70
7B33LQ1	6.16	--	4.35	21.6	22.6	20.36	--	4.81	11.23	--	--	5.79	5.4	0.83	--

TABLE III   In %   SPECTROCHEMICAL RESULTS

Spec. No.	Mg	Ti	Mn	Ag	As	B	Ba	Be	Cl	CO	Cr	Cu
77B42LQ1	3.0	.51	.10	<.0005	<.20	<.0050	.12	<.0003	<.020	.0019	.0063	.0083
77B43LQ1	1.4	.26	.040	<.0005	<.20	<.0050	.098	<.0003	<.020	<.0010	.0018	.0080
77B44LQ1	1.6	.27	.055	<.0005	<.20	<.0050	.092	<.0003	<.020	.0011	.0026	.0010
77B45LQ1	1.4	.63	.15	<.0005	<.20	<.0050	.030	<.0003	<.020	.0015	<.0005	.0041
77B46LQ1	3.7	.58	.12	<.0005	<.20	<.0050	.13	<.0003	<.020	.0031	.014	.010
77B47LQ1	0.095	.046	.0072	<.0005	<.20	<.0050	.082	<.0003	<.020	<.0010	<.0005	.0014
77B48LQ1	1.1	.22	.037	<.0005	<.20	<.0050	.077	<.0003	<.020	.0011	.0020	.0039
77B49LQ1	1.7	.31	.058	<.0005	<.20	<.0050	.011	<.0003	<.020	<.0010	.0023	.0010
77B50LQ1	2.3	2.4	.17	<.0005	<.20	<.0050	.027	.00034	<.020	.0046	.0047	.077
77B51LQ1	1.5	.24	.044	<.0005	<.20	<.0050	.097	<.0003	<.020	<.0010	.0016	<.0007
77B52LQ1	1.9	2.3	.14	<.0005	<.20	<.0050	.030	<.0003	<.020	.0046	.0048	.076
77B53LQ1	4.2	.67	.14	<.0005	<.20	<.0050	.11	<.0003	<.020	.0032	.020	.0042

	La	Mo	Ni	Pb	Sb	Sn	Sr	V	Y	Yb	Zn	Zr
77B42LQ1	<.010	<.0050	.0024	<.070	<.050	<.020	.11	.016	<.0040	<.0040	<.020	.016
77B43LQ1	<.010	<.0050	.0024	<.070	<.050	<.020	.069	.051	<.0040	<.0040	<.020	.018
77B44LQ1	<.010	<.0050	.0024	<.070	<.050	<.020	.082	.0078	<.0040	<.0040	<.020	.019
77B45LQ1	<.010	<.0050	.0024	<.070	<.050	<.020	.035	.014	<.0040	<.0040	<.020	.022
77B46LQ1	<.010	<.0050	.0036	<.070	<.050	<.020	.13	.019	<.0040	<.0040	<.020	.023

TABLE III (Continued)

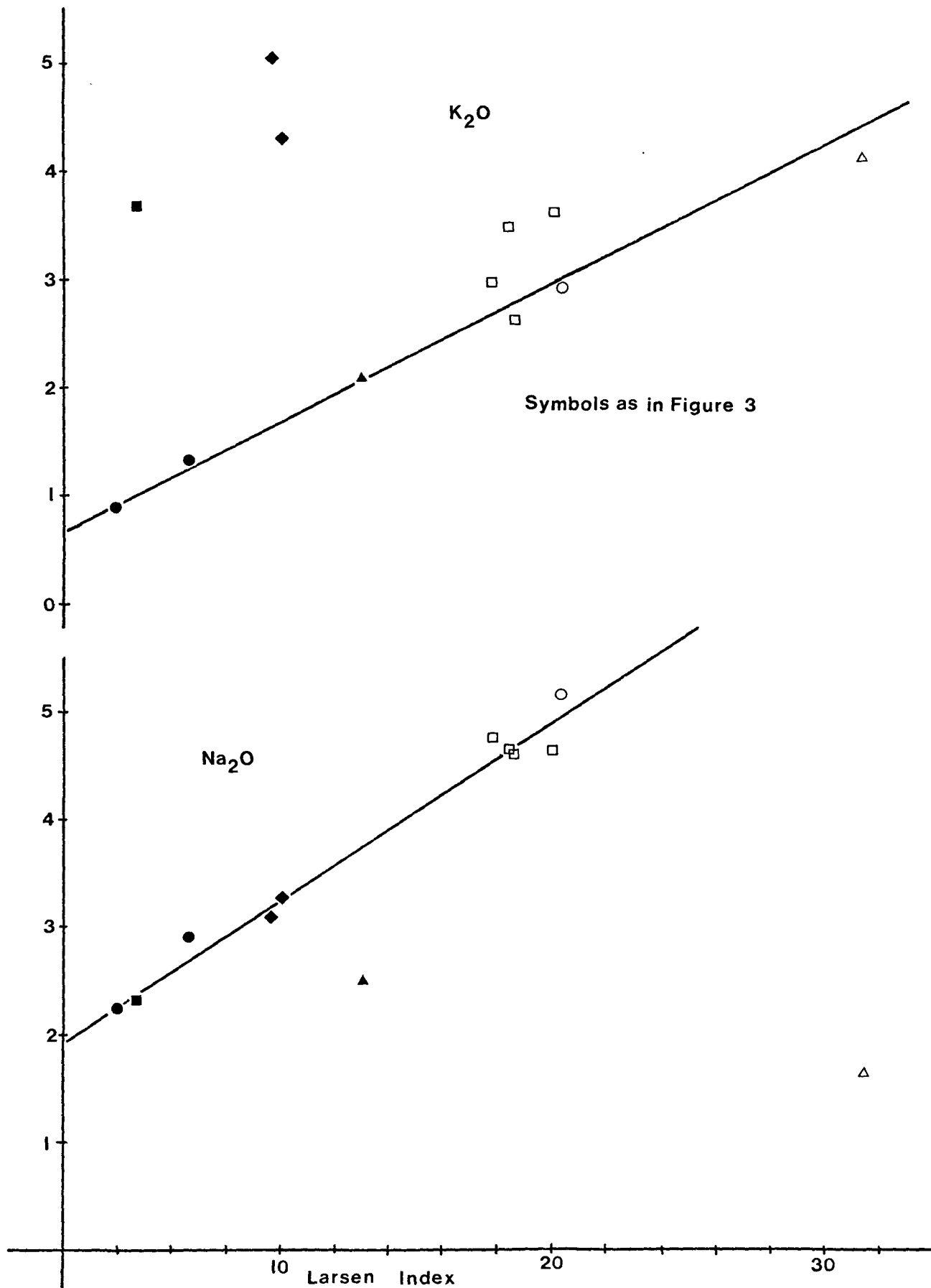| Species No.	La	Mo	Ni	Pb	Sb	Sn	Sr	V	Y	Yb	Zn	Zr
77B47LQ1	<.010	<.0050	<.0010	<.070	<.050	<.020	.011	.0025	<.0040	<.0004	<.020	.015
77B48LQ1	<.010	<.0050	.0013	<.070	<.050	<.020	.0501	.0065	<.0040	<.0004	<.020	.019
77B49LQ1	<.010	<.0050	.0010	<.070	<.050	<.020	.086	.0072	<.0040	<.0004	<.020	.018
77B50LQ1	<.010	<.0050	.0088	<.070	<.050	<.020	.028	.048	.0076	.00060	<.020	.044
77B51LQ1	<.010	<.0050	<.0010	<.070	<.050	<.020	.048	.0058	<.0040	<.0004	<.020	.014
77B52LQ1	<.010	<.0050	.0064	<.070	<.050	<.020	.040	.040	.0065	<.0004	<.020	.046
77B53LQ1	<.010	<.0050	.0038	<.070	<.050	<.020	.11	.021	<.0040	<.0004	<.020	.019

Figure 18

Figure 18   38

Symbols as in Figure 3

Figure 18   38

K_2O

Symbols as in Figure 3

Na_2O

Larsen Index

Figure 18   38
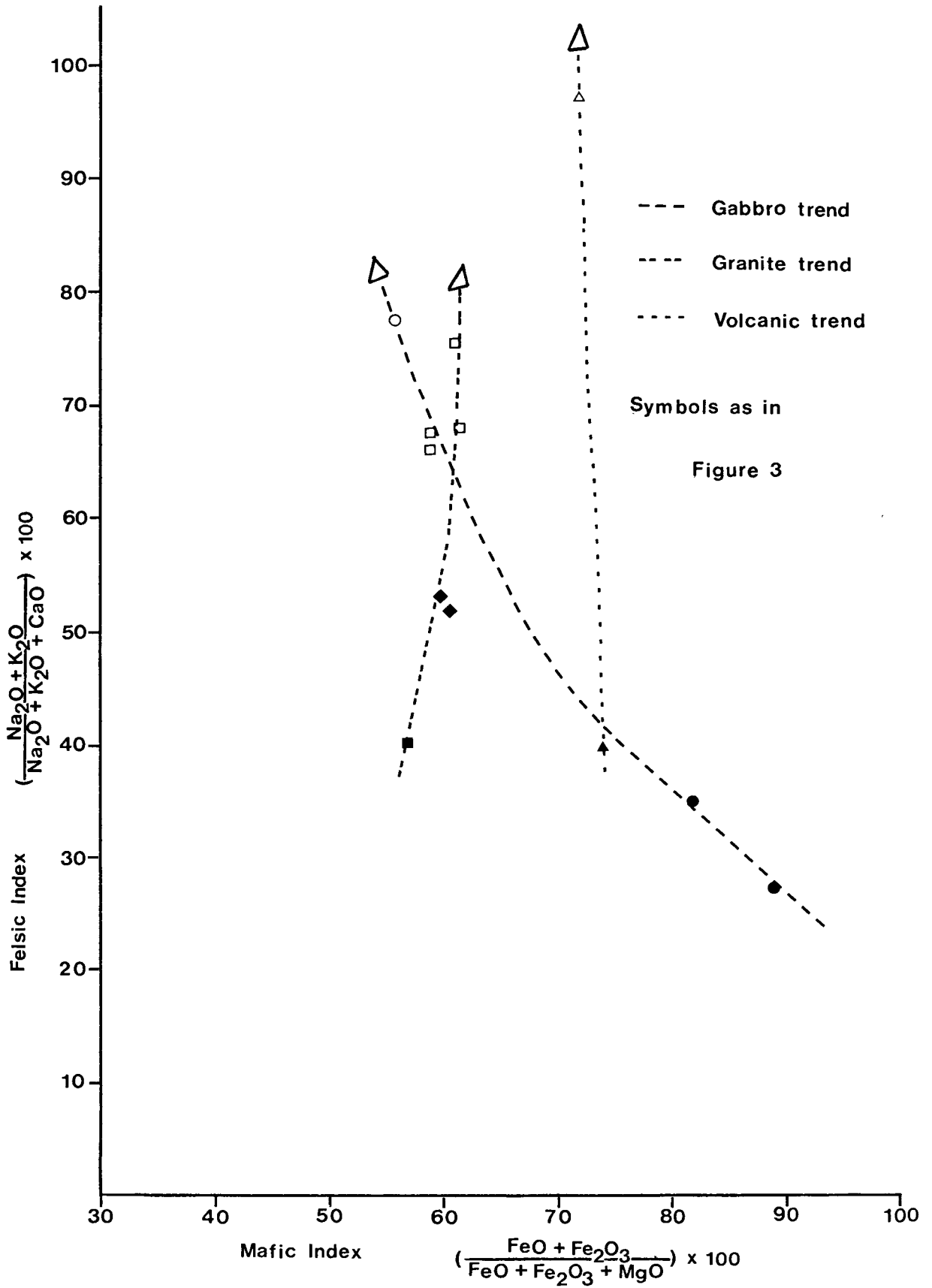

Symbols as in Figure 3

Al_2O_3

Larsen Index

Figure 19   39

Figure 19

FeO + Fe$_2$O$_3$

Symbols as in Figure 3

K$_2$O + Na$_2$O   MgO
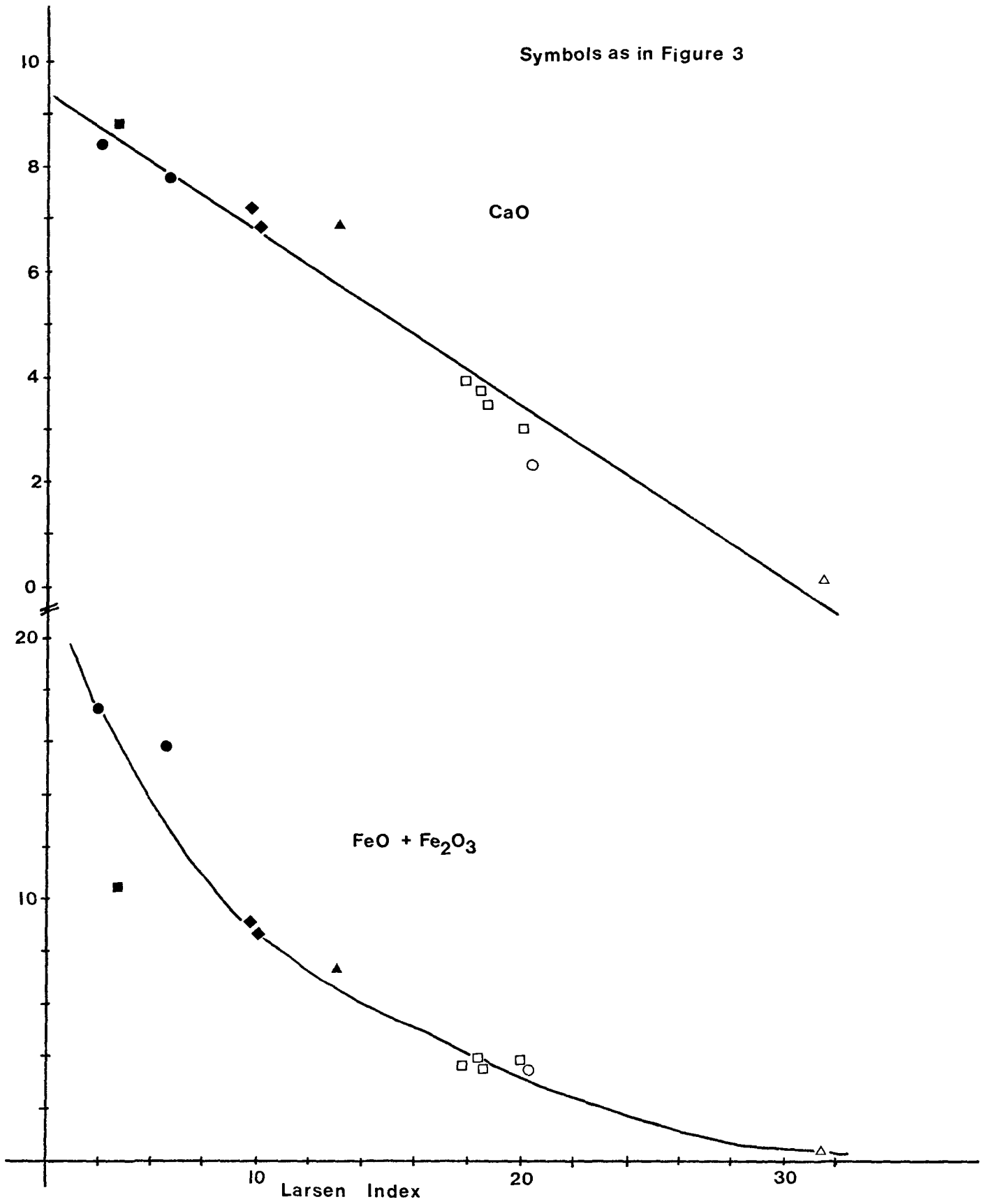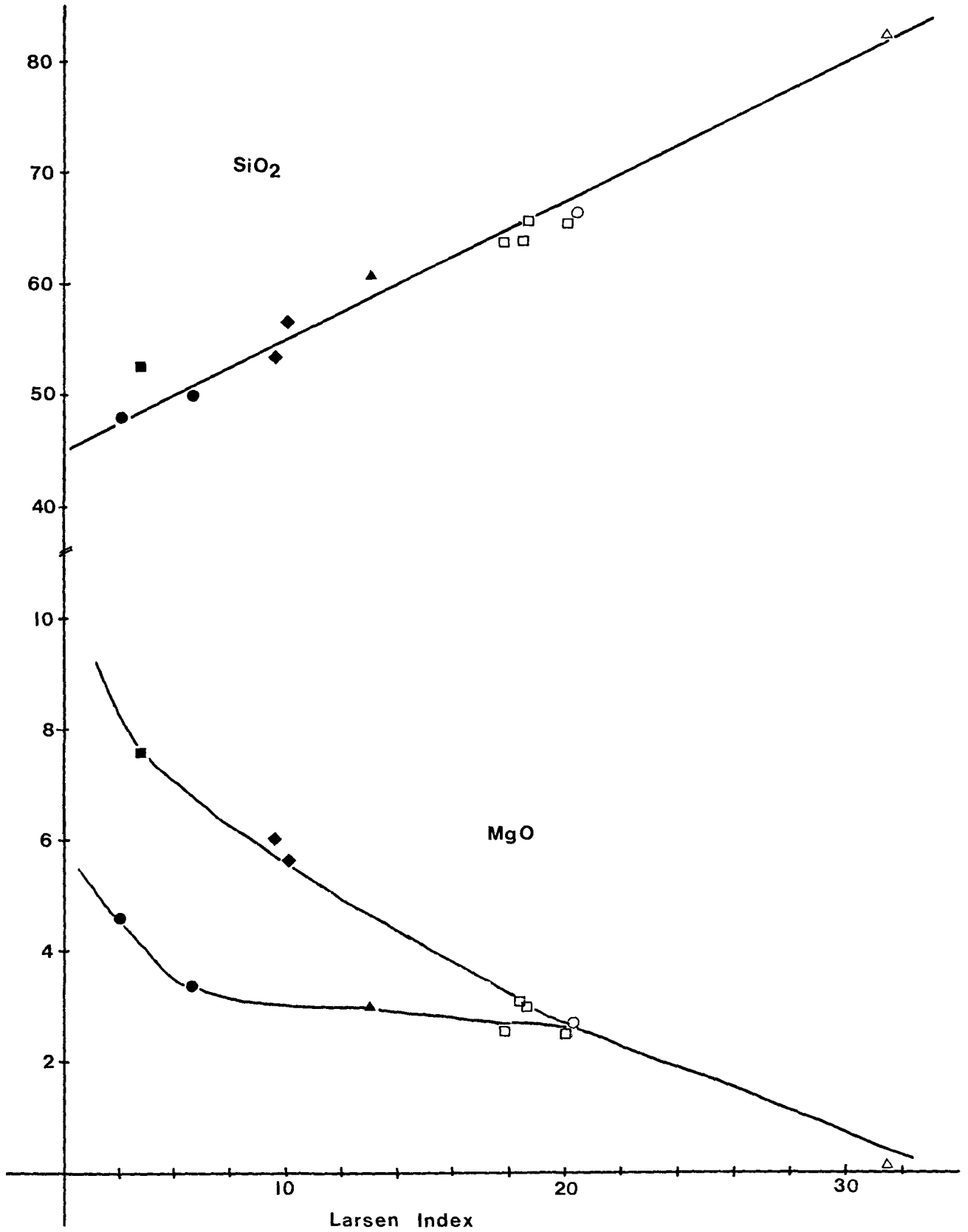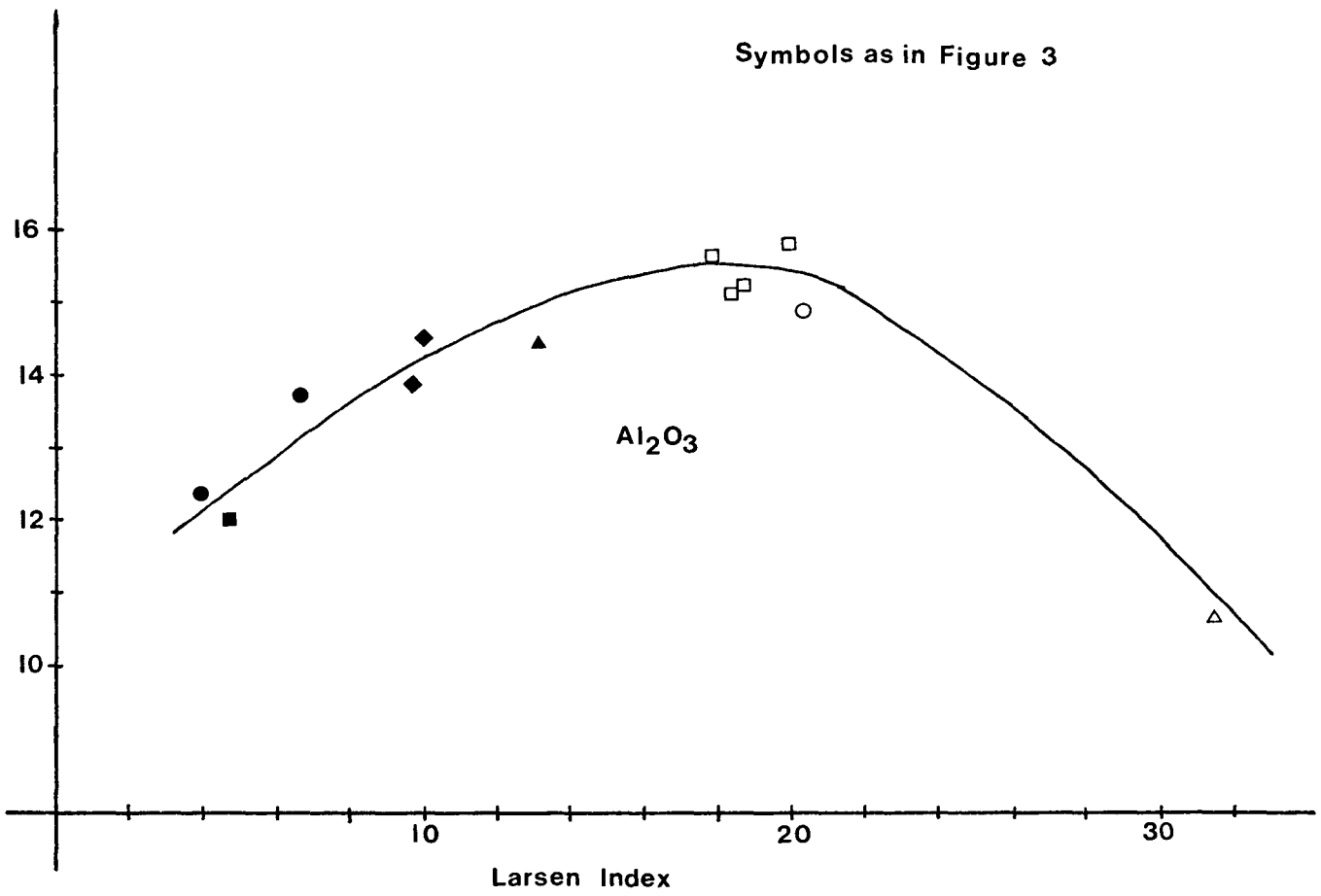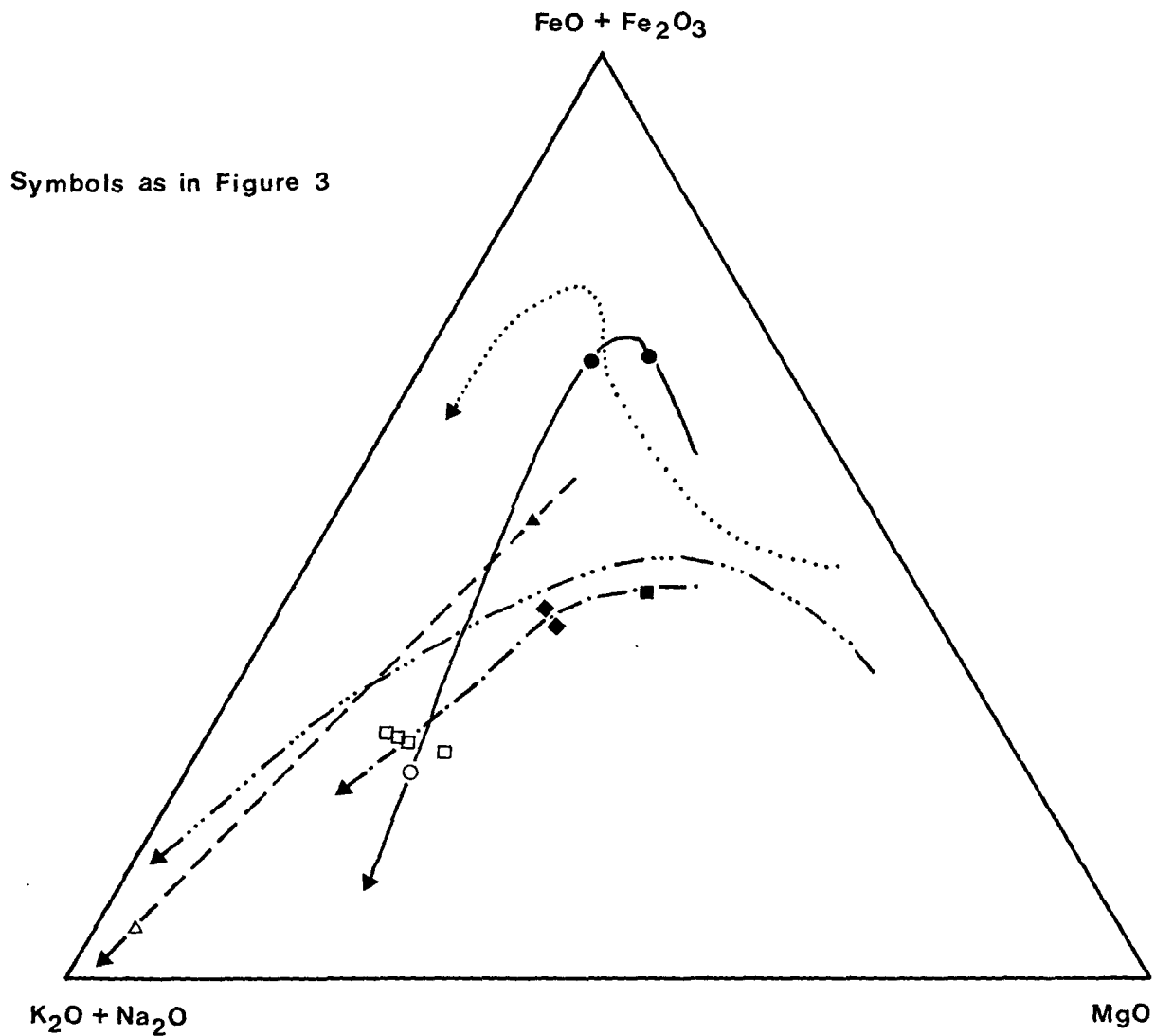
$\cdot - \cdot -$ Granite trend

$- - - -$ Volcanic trend

$———$ Gabbro trend

$\cdots\cdots$ Palisades trend

$— \cdots —$ Calc-Alkaline Cascades trend

Figure 20   40

Figure 20

Figure 21 .41

ACF Diagram
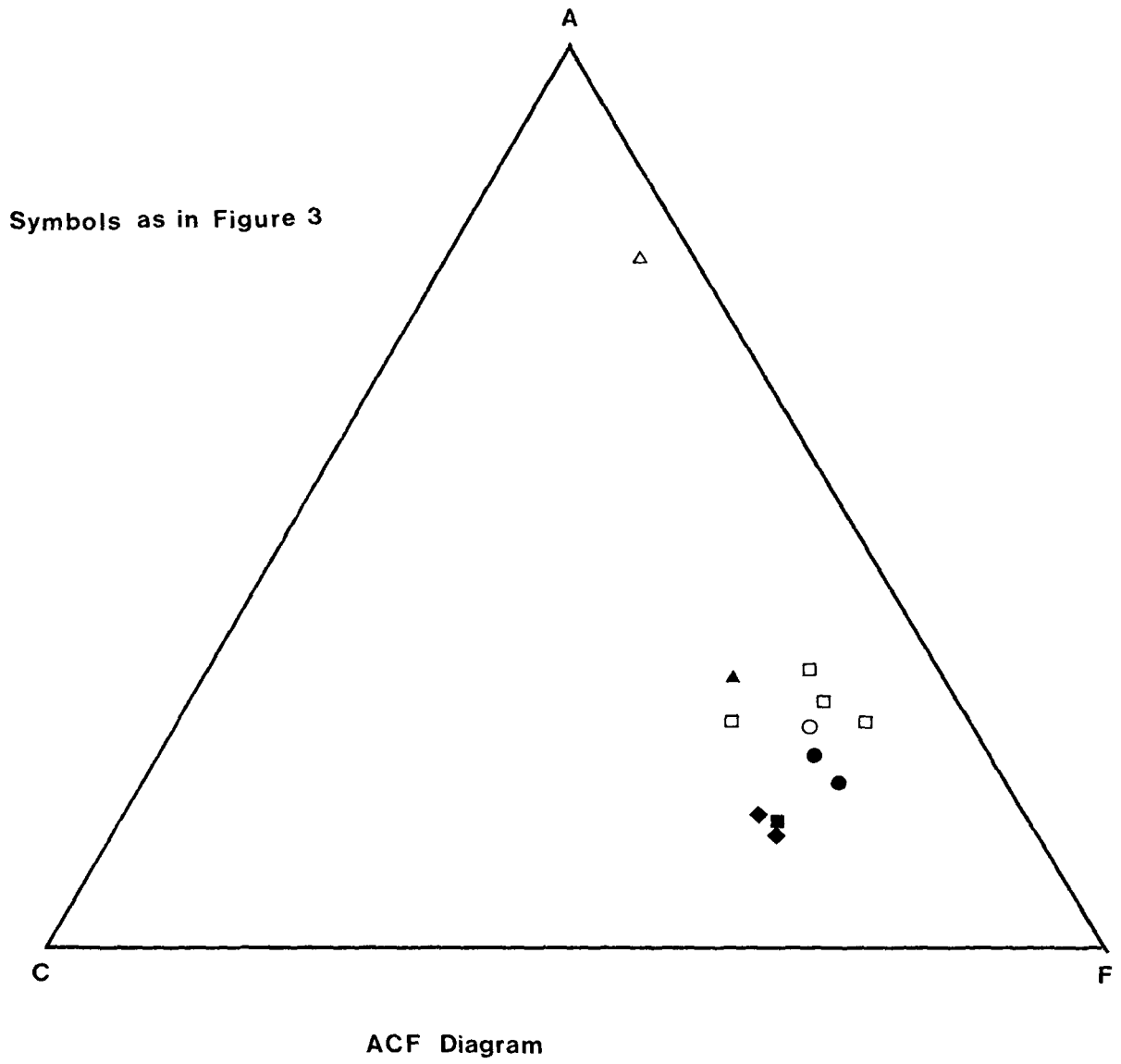
CHAPTER V

GENESIS OF THE ZONED GABBRO-QUARTZ GABBRO DYKE

(1) Introduction

Chapter Three has already dealt with the matter of the petrology
of the zoned gabbro-quartz gabbro dyke in considerable detail. The
purpose of this chapter is to further discuss the matter of the formation
of this zoning.

To simplify the problem, the rock body under consideration may be
thought of as a vertically standing plate of uniform width (69 meters;
190 feet). It is diabasic in composition, showing no traces of flowage
features in either hand specimen or thin section. Thus, the assumption
is made that the dyke was formed by a single injection of magma, which
was then left to cool slowly. In this model, simple symmetrical cooling
is assumed to have proceeded from the margins towards the centre at a
uniform rate.

The major mineral species recognized in these dyke rocks are
pyroxene and plagioclase, and in general, they are found to have formed
in a subophitic texture. Towards the centre of the dyke however, the
plagioclase laths become very altered; the twin planes lose their crisp
outlines and become very difficult to determine compositionally. It
has also been noted that with continued cooling, certain areas of the
dyke show an increasing proportion of plagioclase and quartz crystallized
in the form of myrmekite, signifying late stage cooling.

- 42 -

One specimen (77B33LQ1) is of particular interest in that it is taken from the chilled margin of the gabbroic phase of the dyke where it sits in contact with the adjacent quartz monzodiorite unit. The information gained from the study of naturally quenched basaltic selvages such as this are important in that they give specific details of the nature, amount, and chemical composition of the included phenocrysts (Walker, 1957). These data show very clearly how far crystallization had proceeded at the time of emplacement of the dyke. It may also be assumed that the chilled margin of the dyke represents the same chemical composition as that of the central portion of the dyke at the time of its initial emplacement (Walker, 1957).

(2) Modal Variations within the Dyke

Modal analyses have been performed on seventeen thin sections, which are representative specimens spanning the entire width of the dyke. Sample spacing ranges from 0.5 m to 11 m, but averages approximately 3 metres. The results of these analyses are tabulated in Table IV, and the variations in modal percentages of plagioclase, pyroxene, opaque oxide, and myrmekite across the width of the dyke are plotted in Figure 22.

Under the assumption of a cooling rock body of finite but constant thickness and infinite depth, one would expect to observe a symmetrical distribution of mineral species across it. It may be anticipated that this would take the form of either a gradual increase or decrease in the abundance of any given mineral towards the centre of the dyke. Figure 22 indicates that this is not the case here. Instead of smooth variations between high and low modal abundances, the results are observed to fluctuate

cyclically between these two extremes.

Of the four particular minerals under study, the variations observed for the plagioclase and pyroxene are the most interesting and unusual. Since between them these two minerals comprise close to 80-90% of the bulk composition of the dyke rocks, they would be expected to delineate the cooling history of the intrusion quite clearly.

The first observation of note is that neither plagioclase nor pyroxene displays the anticipated smoothly varying distribution trends of a simple dyke. Upon closer examination, however, it can be seen that, for the most part, the wildly fluctuating trends of these two minerals are related. Throughout the central portions of the dyke, the relationship is antipathetic, such that where pyroxene is abundant, plagioclase is relatively scarce and vice versa. But for the marginal three or four samples from either edge of the dyke, the variations between pyroxene and plagioclase are extremely sympathetic.

It is immediately evident from the preceeding discussion that the crystallization of this system is not following the normally expected trends of a simple dyke. Some external agent must be influencing the system such that it deviates from the norm. One possible factor of considerable influence is the effect of changing water pressure during the crystallization of a magma.

It is known that the presence of water in a magma can have a profound effect on its physical properties, and can be important in influencing its evolutionary trend. Hamilton and Anderson (1967) states that when present in a magma, water will effectively (1) decrease its viscosity, (2) lower the temperature at which crystallization will begin and end,

(3) tend to favour the crystallization of hydrous minerals, and (4) control the rate of the fall of the partial pressure of oxygen with temperature. Thus, among other things, changes in water pressure within a magma can induce shifts in the position of boundary curves between mineral phases (Hamilton and Anderson, 1967).

Consider the ternary system Diopside-Albite-Anorthite which, to a first approximation, is a good representative model of this dyke. An assumption must first be made, however, of considering all the pyroxene in the system as diopside. With this assumption in mind, the modal compositions of the dyke rock specimens can be plotted within the ternary diagram of the system (see Figure 23). The boundary curve between the pyroxene and plagioclase primary phase fields is shown in Figure 23 for conditions of one atmosphere pressure and a liquidus temperature of 1298°C (Lindsley and Emslie, 1966). But Yoder (in Lindsley and Emslie, 1966) suggested that high water pressures in the Di-Ab-An system might move the water saturated diopside-plagioclase boundary curve towards the plagioclase region; specifically towards the anorthite corner. This shift in the position of the boundary curve, resulting from an increase in water pressure, coupled with an increase in temperature, is only valid for pressures of up to 32 kilobars (Yoder, 1964), after which point anorthite breaks down and the diopside-anorthite join is no longer stable. Figure 24 (after Lindsley and Emslie, 1966) indicates the manner in which the boundary curve shifts with increasing water pressure up to 20 kilobars. Although the pressures attained in the rock system under study here do not reach magnitudes as great as 20 kilobars at any time, Figure 24 is useful in that it indicates the general trend of the boundary curve move-

ment as water pressure is increased. From this Figure it is also apparent that basaltic magmatic compositions which lie in the plagioclase primary phase field near the boundary curve at low water pressures, will lie in the pyroxene primary phase field at higher water pressures. The removal of the crystallized pyroxene as water pressure increases might tend to drive the composition of the residual magmatic liquid towards that of plagioclase.

The changes in the position of the Di-An boundary curve resulting from changes in water pressure discussed above can, in theory, be used to attempt an explanation of the erratic behaviour of pyroxene and plagioclase in Figure 22.

As discussed before, the samples taken across the width of the dyke can be subdivided into two sub-phases; a marginal phase, and a central phase. If the data from Figure 23 are replotted such that Figure 25 shows only the marginal phases, and Figure 26 the central region, the crystallization path of the dyke becomes somewhat more lucid. The marginal phases show compositions in the pyroxene primary phase field, which fall in two clusters; one for each margin of the dyke. A definite crystallization path is followed by the compositions of the rocks of the central region of the dyke (Figure 26), which has its origin in the pyroxene primary phase field of the diagram. As cooling continues, and crystallization proceeds, the rock compositions become increasingly depleted in diopside and enriched in plagioclase, while the plagioclase compositions seem to telescope from higher and lower An values along the western and eastern margins of the dyke respectively, to a final value of approximately An_{50} at the centre of the dyke. The lowest point in Figure 26

represents a composition from near the centre of the dyke, which is also at the lowest temperature. As indicated by Lindsley and Emslie (1966) previously, continuously increasing water pressure will shift the boundary curve towards the anorthite corner, and a removal of the solid pyroxene crystals from the melt will drive the residual liquid towards plagioclase, as observed in Figure 26.

Thus, in summary, fluctuations in the modal percentages of pyroxene and plagioclase across the dyke, as shown in Figure 22, may be accounted for by any one of three possible mechanisms. First is the possibility that these fluctuations are the results of fractional crystallization of the magma. Thus, when large amounts of pyroxene are crystallized, it must be compensated for by a corresponding lack of plagioclase, such that the bulk composition remains relatively constant. It can be seen, however, that this explanation does not hold, because if this were so, one would expect that with cooling, the rock composition would follow the boundary curve until reaching its final composition, and not continue down into the plagioclase primary phase field as it does in Figure 26. A second hypothesis is that the position of the Di-An boundary curve fluctuates under the influence of changing water pressure in the melt. This shift in position of the curve may result in fluctuations in the amount of pyroxene or plagioclase produced as the composition alternates between the pyroxene and plagioclase primary phase fields. Thus, the results of Figure 22 can be accounted for. However, the extremely high water pressures necessary to achieve these boundary shifts are not feasible in a natural dyke of this sort, so this theory must be totally rejected. A third and final hypothesis is the possibility that this dyke may have

resulted from more than one period of injection. Evidence for multiple injection is not apparent from field work and mapping, yet it is suggested by the fact that the dyke shows two separate cooling trends within it. A distinct marginal zone is observed in which pyroxene and plagioclase modes are sympathetic, while an inner region representing the more acidic core of the dyke, shows these two mineral phases as being distinctly antipathetic. Broad trends of increasing plagioclase and decreasing pyroxene can be envisaged as applying to Figure 22 if the dyke is considered as resulting from multiple injection, in which case the marginal samples can be ignored. In light of the data presented here, the third alternative appears the most likely, despite the lack of any convincing field evidence.

(3) <u>Crystal Size Variation</u>

It is a well-known fact that in small intrusive igneous bodies, such as dykes, the grain size of the individual crystals is a function of distance from the contact of the body. Differences in cooling rates across such a body generally result in a much finer grain size along the margins than at the centre of the body (Winkler, 1949). In an attempt to verify these statements and thereby obtain some statement of the cooling history of the dyke, the thin sections were analyzed with respect to grain size. It was felt by the author that the plagioclase laths would give the best indication of relative crystal growth rates with respect to time. Thus, the visible area of the smallest size fraction of plagioclase laths was measured in each thin section. When these results were plotted, however, the expected smooth curve showing grain size increasing towards the centre was not observed. As the method of measuring grain

size with the Shadowmaster (McMaster University facility) was not very accurate, and the dyke under investigation a mere 69 meters wide, the study of this aspect of the dyke was abandoned.

(4)   Pyroxene Ratios

The Pyroxene Ratio is defined by Walker (1957) as

$$P.R. = \frac{Pyroxene \times 100}{Pyroxene + Plagioclase}$$

and is considered by him to be an important criterion directly related to the texture and mineral composition of the rock. A histogram of pyroxene ratios is plotted in Figure 27 for the gabbroic dyke rocks. Walker does not define an absolute scale with which to compare the pyroxene ratios of various different ophitic and subophitic intrusions. It appears to be his belief that ophitic rocks generally tend to have a slightly higher pyroxene ratio than that observed in subophitic rocks. The average pyroxene ratio of the dyke studied here, which has a subophitic texture, is 39.06. This value is comparable with those generally found by Walker (1957) for rocks of a similar composition and texture.

TABLE IV   Modal Analyses across Gabbro/Quartz Gabbro Dyke

Sample No.	Dist. (ft)	Plag.	Px	Ox	Myrm	Biot.	Qu
32-2	4.	47.4	37.8	10.3	3.4	---	1.0
13-1	24.	39.0	29.1	7.0	13.3	1.1	10.3
51-1	28.	60.8	13.9	1.0	--	---	24.3
50-1	36.	46.1	39.3	9.6	3.0	0.2	1.8
41-7	38.	38.6	33.2	11.8	13.2	---	3.1
41-6	56.	42.0	27.2	5.5	15.4	2.5	7.4
41-5	76.	52.8	25.9	5.5	4.4	2.1	9.4
9-1	80.	56.9	20.7	6.1	--	4.1	12.4
41-4	102.	48.9	27.1	5.1	1.8	1.1	15.9
41-3	138.	60.6	19.7	7.0	7.5	1.4	3.7
8-3	146.	49.3	29.2	11.9	6.9	0.4	2.3
41-2	154.	42.4	40.1	8.9	5.3	0.6	2.7
8-2	160.	48.1	27.8	9.2	9.9	0.5	4.5
41-1	168.	46.1	41.1	10.1	1.8	---	0.5
8-1	174.	41.8	33.1	10.7	11.2	1.0	2.4
52-1	178.	47.4	35.9	8.3	6.0	0.3	2.1
33-1	190.	7.2	7.2	85.6% vfgr. groundmass			

Figure 22 51

Figure 22

Figure 22   51

Figure 22

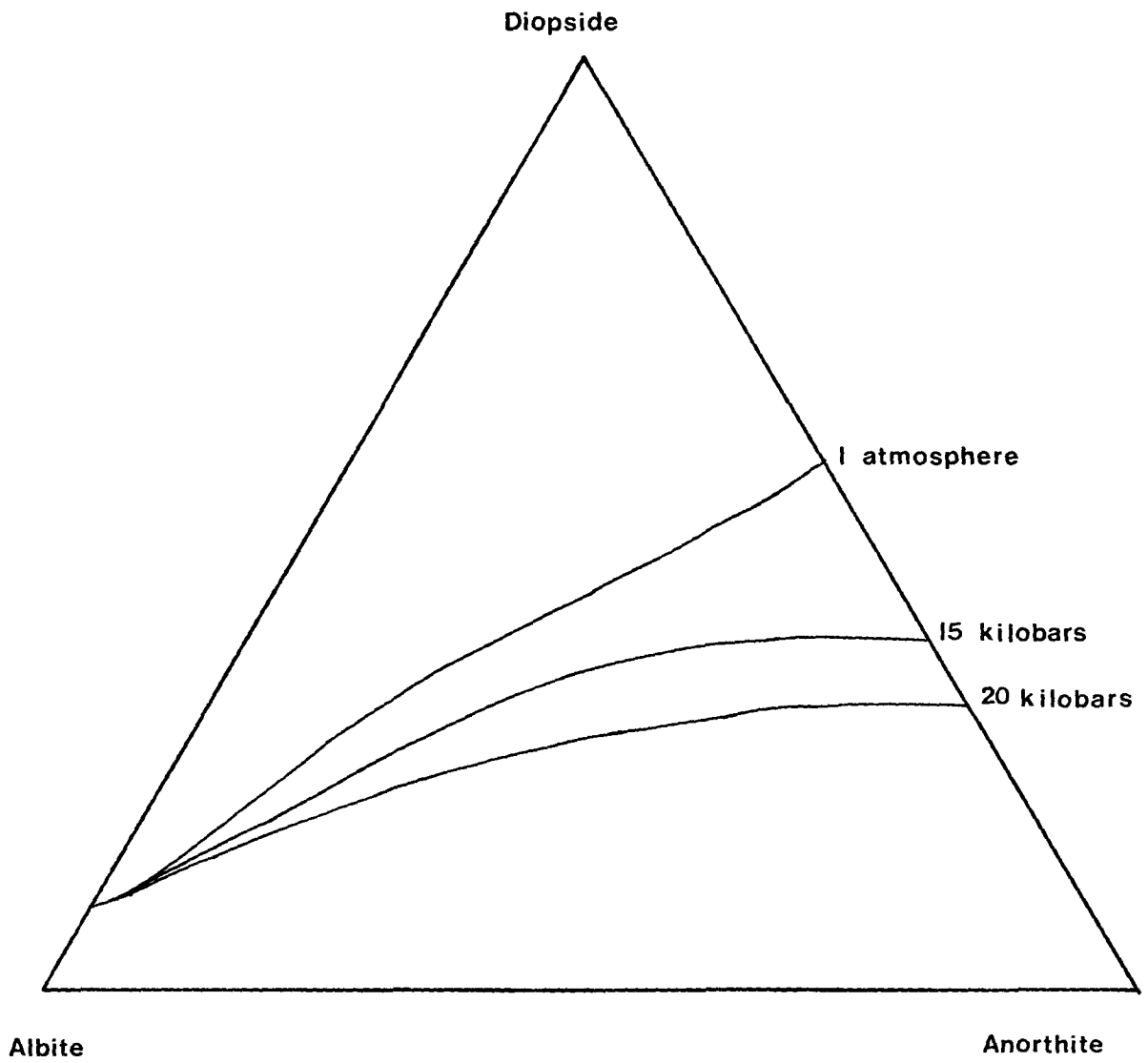Figure 23   52
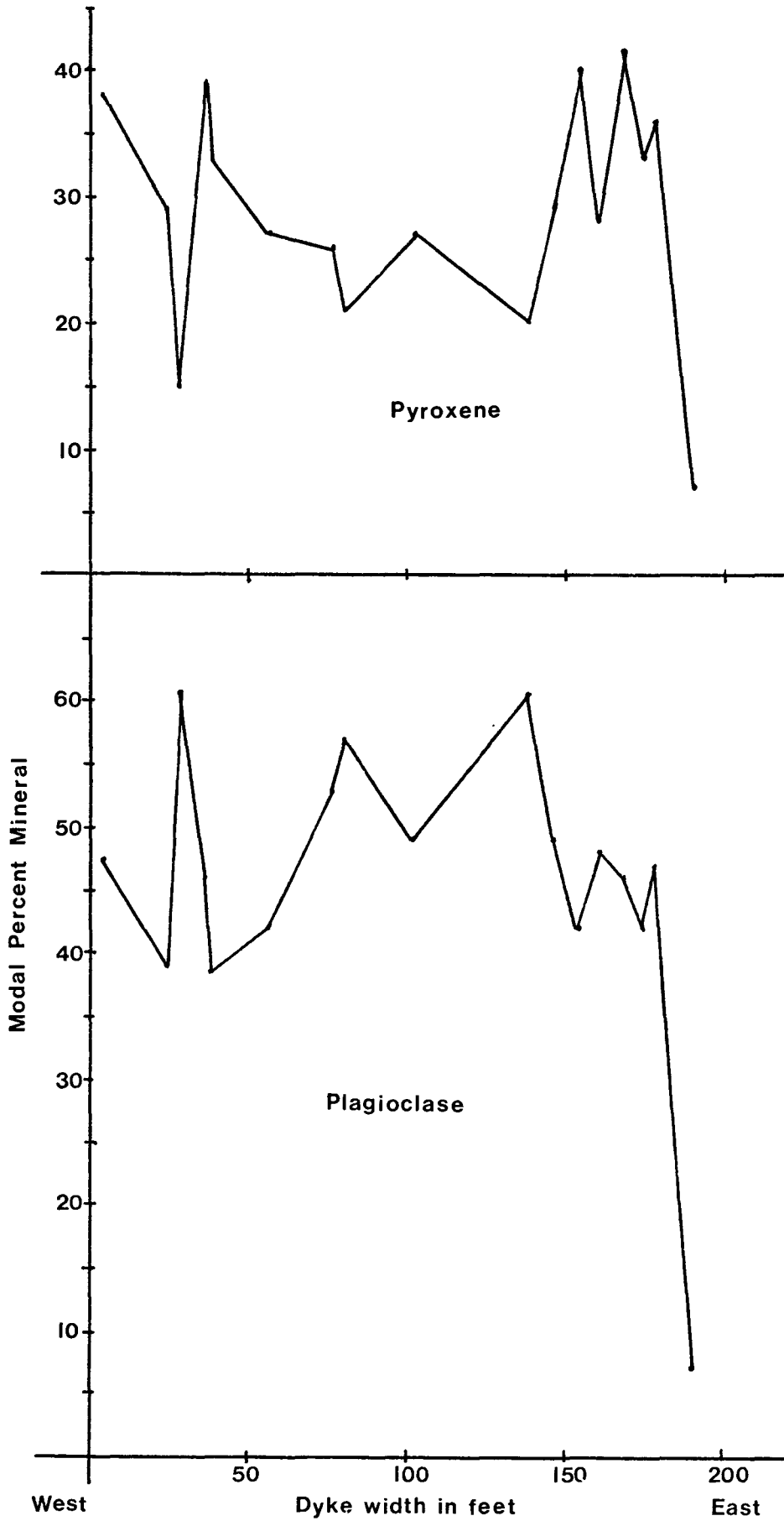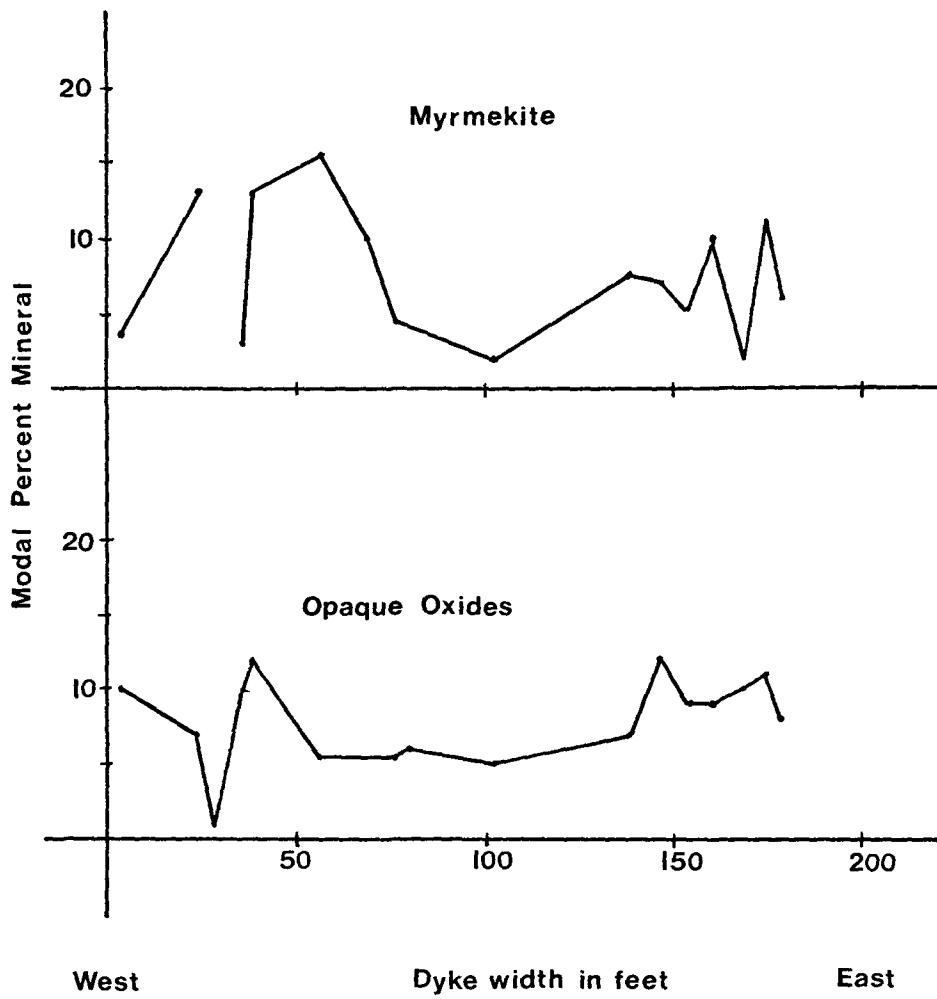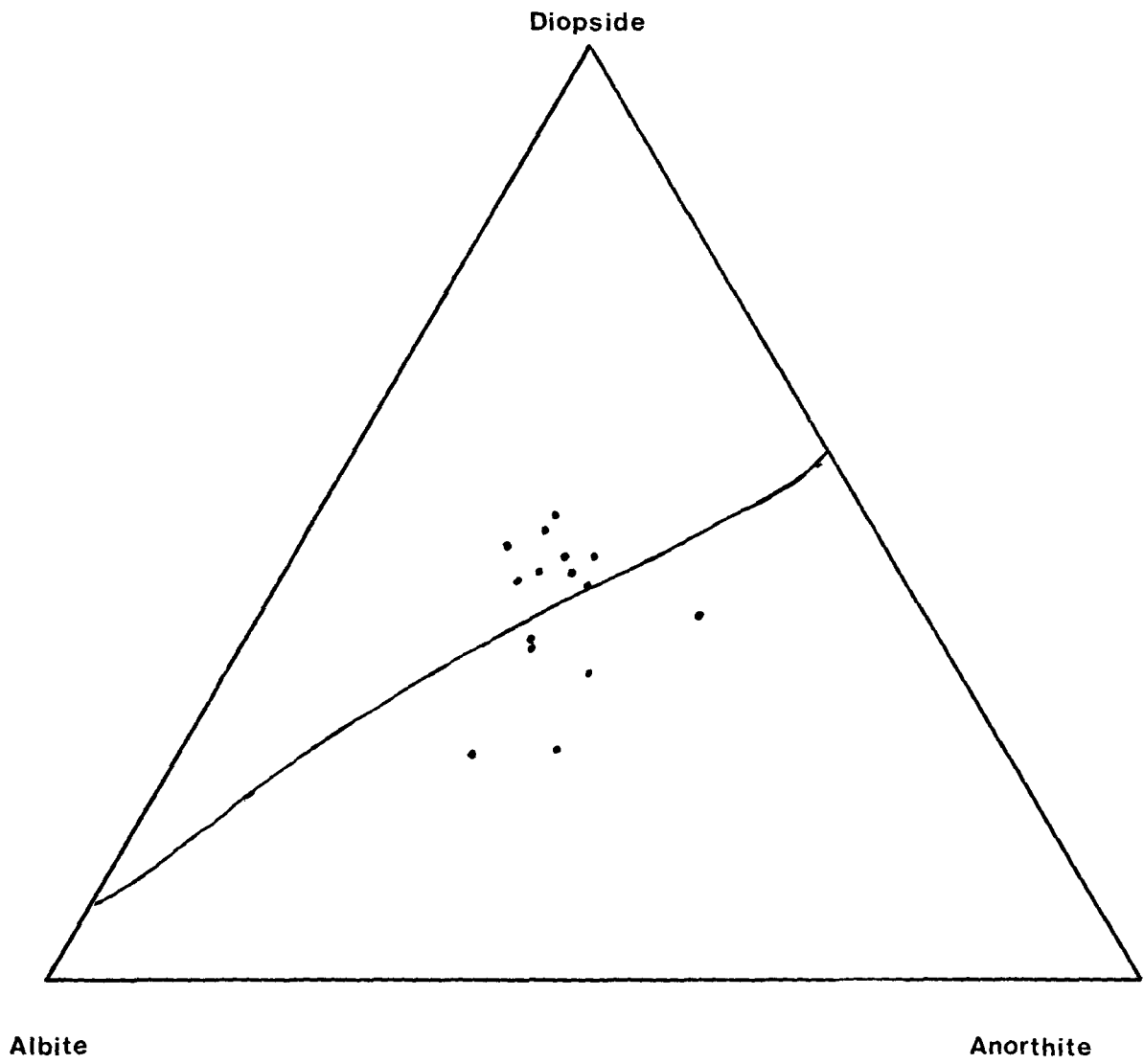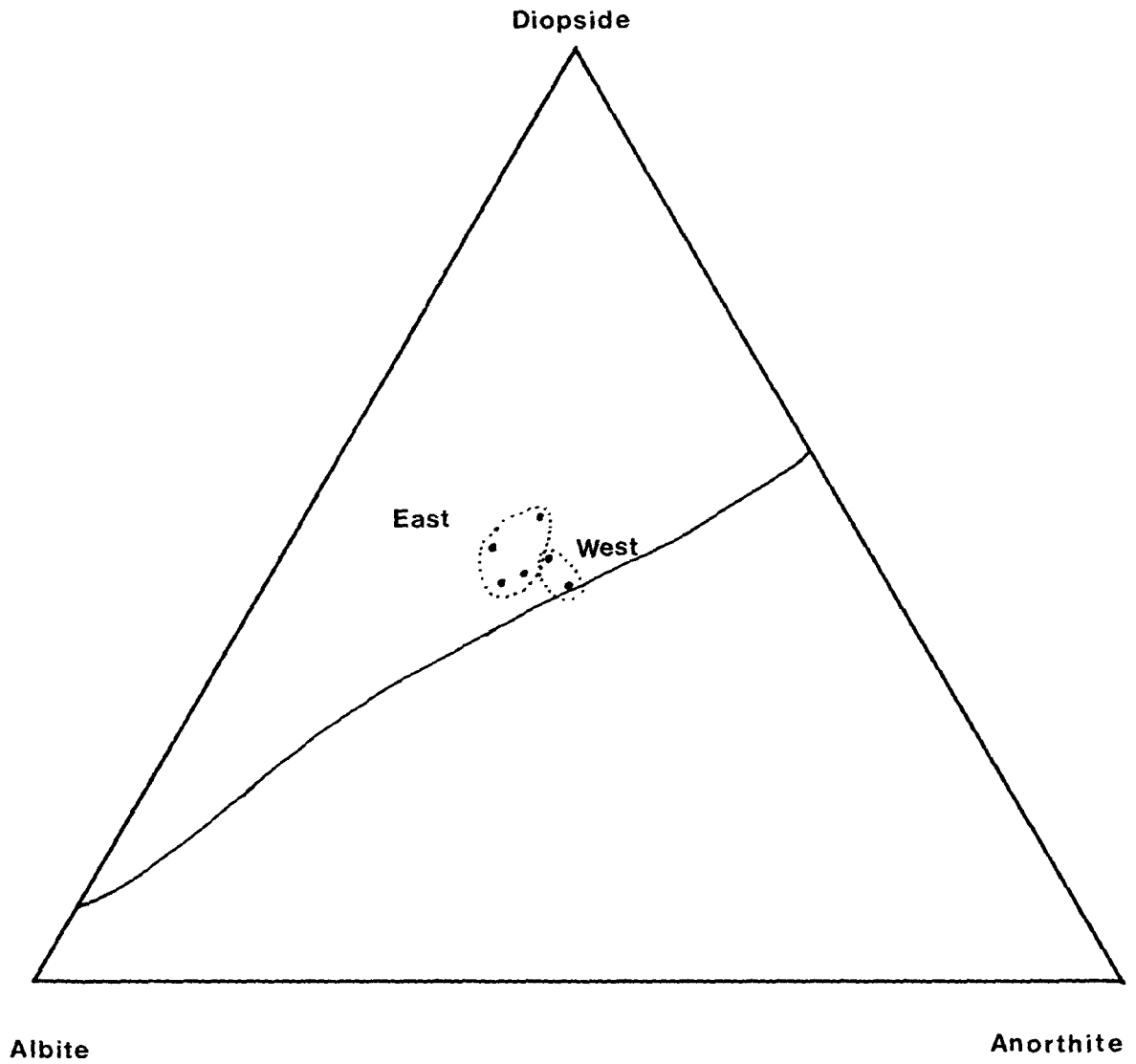

Di–Ab–An Ternary Phase Diagram

Figure 24   53

Boundary Curve Shifts with Increasing Pressure of Fluid
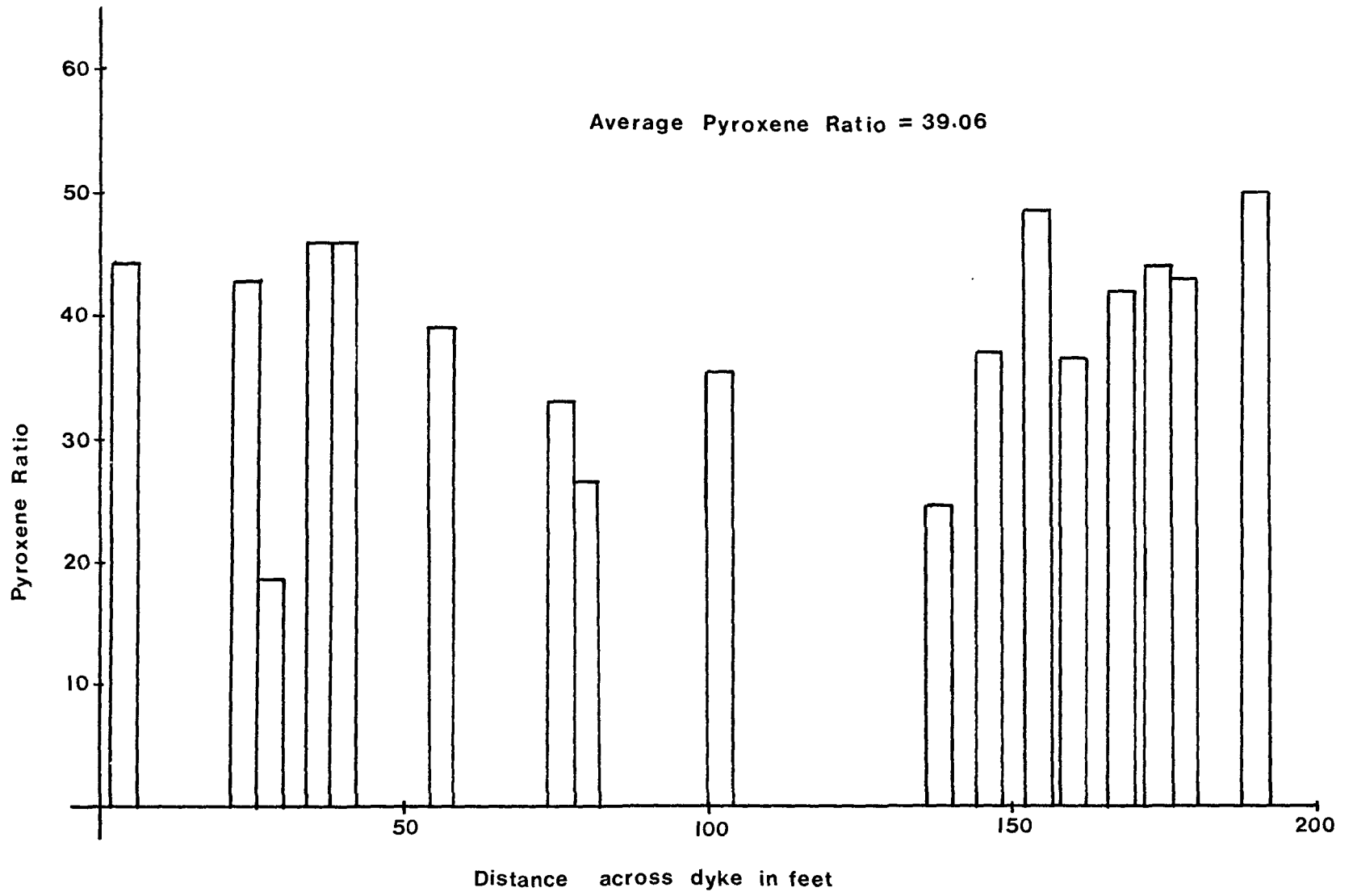
Figure 25

Marginal Zones

Figure 26

Central Zone
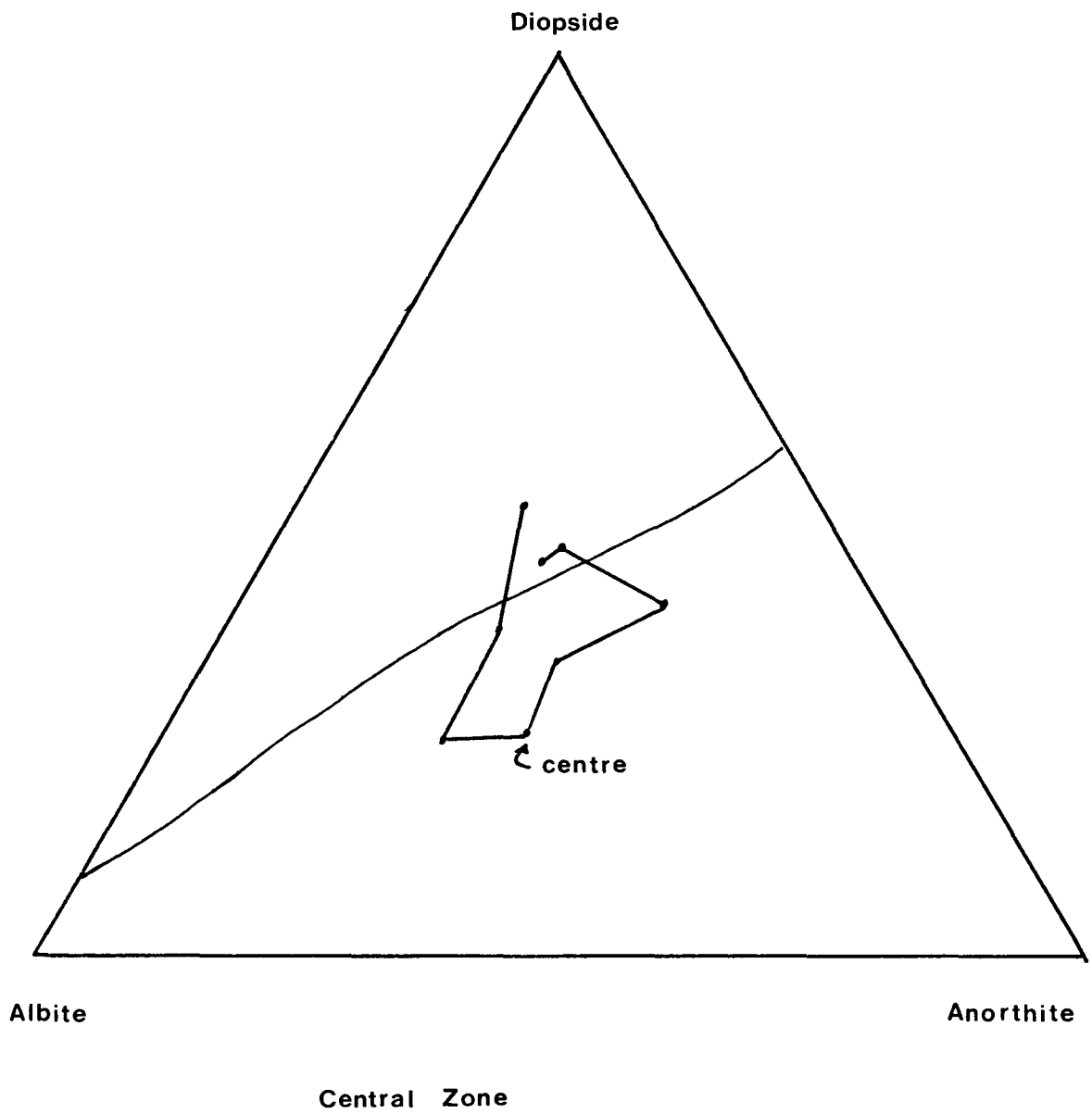
Figure 27

CHAPTER VI

CONCLUSIONS

The igneous intrusives mapped by the author intrude a felsic volcanic pile of Archean age, which forms part of the Back River Volcanic Complex. This volcanic pile consists dominantly of pyroclastic andesites, which were later invaded by rhyolitic domes along concentric ring fractures marginal to the volcanic pile (Lambert, 1978). The intrusive granites show signs of having undergone fractional crystallization. These are cut by a much younger zoned gabbroic dyke.

The sequence of events which produced these features may be summarized as follows:

(1) Deposition of pyroclastic andesites on top of an emergent volcanic pile.

(2) Rhyolite flows out from radial ring fractures.

(3) Three granitic units are then intruded into the volcanics. These are thought by the author to represent successive distillations from a single body of parent magma. Field relations suggest and chemical studies support this hypothesis, in the fact that as fractional crystallization and subsequent injections proceed, the magma becomes progressively depleted in ferromagnesian minerals and enriched in alkalis (as indicated by the AFM diagram). The signature of all of these three intrusive phases is the presence of distinctive hornblende phenocrysts, which is another indication that they may

share a common parentage.

(4) In order of decreasing age, the intrusive units are:

    (i) Hornblende Quartz Syenite

    (ii) Granite

    (iii) Quartz Monzodiotire

Field relations, physical appearance, and chemistry indicate that
the hornblende quartz syenites and granites may in fact represent
the same rock body. This has not been established conclusively,
although these two granitic units are frequently found to plot in
the same vicinity on chemical diagrams, and their mineralogy is
not markedly different.

(5) All three granitic units, as well as the rhyolites were finally cut
by a zoned gabbro Mackenzie type dyke. At its intrusion, the magma
was approximately 14% crystalline and 86% liquid. This solid phase
consisted of plagioclase and pyroxene in approximately equal pro-
portions, indicating crystallization had commenced at depth before
intrusion. The contact between the dyke and surrounding units is
sharp and almost vertical. Intrusion creates a contact aureole
up to 30 meters wide, which is most visible in the adjacent quartz
monzodiorite unit. Zoning in the dyke is developed during cooling,
such that the subophitic chilled gabbroic margins grade into a
coarser quartz gabbro toward the centre, with granophyric areas
near the core. The zoning may be accounted for by one of three
possible hypotheses:

    (i) fractional crystallization of a single magma

    (ii) marginal injection of magmas from different sources

(iii) changing water pressure in the magma with continued cooling. Although not suggested by field work, the chemical and graphical evidence seems to favour the second hypothesis of multiple injection.

(1) <u>Suggestions for Further Work</u>

(1) Further more detailed study of the Mackenzie type dykes. These are prominent features within the Slave Province, and have been largely ignored in most surveys of the area. Little is known of their petrology and the genesis of their zoning.

(2) Comparison between the granites of this area and other similar necks of granites found within the Complex. These areas are not uncommon and may be related, along with the dykes, to more recent magmatic activity in what are considered inactive volcanic areas.

REFERENCES

--- <u>Plutonic Rocks</u>, Classification and Nomenclature Recommended by the IUGS Subcommission on the Systematics of Igneous Rocks, Geotimes, 1973.

BARAGAR, W.R.A., 1975, <u>Miscellaneous Data from Volcanic Belts at Yellowknife, Wolverine Lake, and James River, N.W.T.</u>, in Report of Activities April to October 1974, Geol. Surv. of Can. Paper 75-1, Part A, pp. 281-286.

CARMICHAEL, I.S.E., TURNER, F.J., VERHOOGEN, J., 1974, <u>Igneous Petrology</u>, McGraw-Hill Book Company, New York.

DOUGLAS, R.J.W., 1970, <u>Geology and Economic Minerals of Canada</u>, Economic Geology Report No. 1, Geol. Surv. of Canada, pp. 72-3, 75, 89.

EHLERS, E.G., 1972, <u>The Interpretation of Geological Phase Diagrams</u>, W.H. Freeman and Co., San Francisco.

FAHRIG, W.F., WANLESS, R.K., 1963, <u>Age and Significance of Diabase Dyke Swarms of the Canadian Shield</u>, Nature, v. 200, pp. 934-937.

HAMILTON, D.T., ANDERSON, G.M., 1967, <u>Effects of Water and Oxygen Pressures on the Crystallization of Basaltic Magmas</u>, in H.H. Hess and Arie Poldervaart (eds.), "Basalts", Interscience, New York, pp. 445-482.

HENDERSON, J.B., 1970, <u>Stratigraphy of the Archean Yellowknife Supergroup, Yellowknife Bay - Prosperous Lake Area, District of Mackenzie</u>, Geol. Survey of Canada, Paper 70-26.

HENDERSON, J.B., 1975, <u>Sedimentological Studies of the Yellowknife Supergroup in the Slave Structural Province</u>, in Report of Activities April to October 1974, Geol. Survey of Canada, Paper 75-1, Part A, pp. 325-330.

IRVINE, T.N., BARAGAR, W.R.A., 1971, <u>A Guide to the Chemical Classification of the Common Volcanic Rocks</u>, Can. Journal of Earth Science, V. 8, pp. 523.

JAEGER, J.C., 1968, <u>Cooling and Solidification of Igneous Rocks</u>, in "Basalts: The Poldervaart Treatise on Rocks of Basaltic Composition", Volume 2, Interscience Publishers, New York.

KERR, P.F., 1959, <u>Optical Mineralogy</u>, third edition, McGraw-Hill Book Company, Toronto.

LAMBERT, M.B., 1976, <u>The Back River Volcanic Complex, District of Mackenzie</u>, in Report of Activities April to October 1975, Geol. Survey of Canada, Paper 76-1, Part A, pp. 363-367.

LAMBERT, M.B., 1977, <u>The Southwest Margin of the Back River Volcanic Complex, District of Mackenzie</u>, in Report of Activities April to October 1976, Geol. Survey of Canada, Paper 77-1, Part A, pp. 179-180.

LAMBERT, M.B., 1978, The Back River Volcanic Complex - A Cauldron Subsidence Structure of Archean Age, in Report of Activities April to October 1977, Geol. Survey of Canada Paper 78-1, Part A, pp. 153-157.

LINDSLEY, D.H., EMSLIE, R.F., 1966, Effect of Pressure on the Boundary Curve in the System Diopside-Albite-Anorthite, in Carnegie Institution Yearbook 66, Geophysical Laboratory, Carnegie Institution, Washington, pp. 479-480.

TURNER, F.J., VERHOOGEN, J., 1960, Igneous and Metamorphic Petrology, second edition, McGraw-Hill Book Company, New York.

WALKER, F., 1957, Ophitic Texture and Basaltic Crystallization, Journal of Geology, V. 65, pp. 1-14.

WILLIAMS, H., TURNER, F.J., GILBERT, C.M., 1954, Petrography: An Introduction to the Study of Rocks in Thin Sections, W.H. Freeman and Co., San Francisco.

WINKLER, H.G.F., 1949, Crystallization of Basaltic Magma as Recorded by Variation of Crystal Size in Dykes, Mineralogical Magazine, V. 28, pp. 557-574.

YODER, H.S., Jr., 1964, Diopside-Anorthite-Water at Five and Ten Kilobars and its Bearing on Explosive Volcanism, in Carnegie Institution Yearbook 64, Geophysical Laboratory, Carnegie Institution, Washington, pp. 82-89.

YODER, H.S., TILLEY, C.E., 1962, Origin of Basalt Magmas: An Experimental Study of Natural and Synthetic Rock Systems, Journal of Petrology, V. 3, Part 3, pp. 342-532.

APPENDIX

Modal Analysis of All Rock Units

Rock Unit & Specimen No.	Plag.	Kspar	Qu	Px	Amph	Ox	Myrm	Biot	Ct.
Gabbro									
77B8LQ1	41.8	--	2.4	33.1	--	10.7	11.2	1.0	--
77B8LQ2	48.1	--	4.5	27.8	--	9.2	9.9	0.5	--
77B8LQ3	49.3	--	2.3	29.2	--	11.9	6.9	0.4	--
77B32LQ2	47.4	--	1.0	37.8	--	10.3	3.4	--	--
77B33LQ1	≐ 35.7	--	≐ 28.5	≐ 35.7	--	--	--	--	--
77B41LQ1	46.1	--	0.5	41.4	--	10.1	1.8	--	--
77B41LQ2	42.4	--	2.7	40.1	--	8.9	5.3	0.6	--
77B41LQ3	60.6	--	3.7	19.7	--	7.0	7.5	1.4	--
77B41LQ7	38.6	--	4.1	33.2	--	11.8	13.2	--	--
77B50LQ1	46.1	--	1.8	39.3	--	9.6	3.0	0.2	--
77B52LQ1	47.4	--	2.1	35.9	--	8.3	6.0	0.3	--
Quartz Gabbro									
77B9LQ1	56.9	--	12.4	20.7	--	6.1	--	4.1	--
77B13LQ1	39.0	--	10.3	29.1	--	7.0	13.3	1.1	--
77B41LQ4	48.9	--	15.9	27.1	--	5.1	1.8	1.1	--
77B41LQ5	52.8	--	9.4	25.9	--	5.5	4.4	2.1	--
77B41LQ6	42.0	--	7.4	27.2	--	5.5	15.4	2.5	--
77B51LQ1	60.8	--	24.3	13.9	--	1.0	--	--	--
Quartz Monzodiorite									
77B43LQ1	50.7	14.3	13.6	--	--	0.2	--	20.0	1.3
77B44LQ1	49.8	16.5	15.3	--	--	--	--	15.9	2.8
77B48LQ1	44.6	13.1	20.4	--	--	0.2	--	15.9	5.7
77B49LQ1	52.8	18.7	13.5	--	--	--	--	12.9	2.1
Granite									
77B32LQ2	14.7	29.3	4.9	47.9	--	3.0	--	--	--
77B32LQ3	15.1	30.1	5.0	15.7	23.7	1.7	--	8.7	--
77B32LQ4	15.2	30.4	5.1	17.3	23.9	3.4	--	3.9	0.8
77B32LQ5	--	43.4	--	15.7	32.0	1.7	--	9.3	--
77B42LQ1	15.7	31.3	5.2	38.9	--	7.9	--	0.9	--
77B46LQ1	10.8	21.7	3.6	26.0	31.0	2.1	--	4.8	--
Hornblende Quartz Syenite									
77B32LQ2	5.5	27.8	22.2	8.0	26.8	2.9	--	6.7	--
77B53LQ1	20.7	26.0	5.2	5.2	32.6	4.2	--	6.1	--

Rhyolite - Modal Analyses not performed.
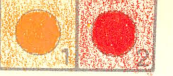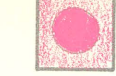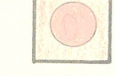
Andesite Tuff - Modal Analyses not performed.
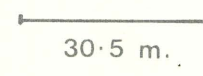
108° 00' W

North
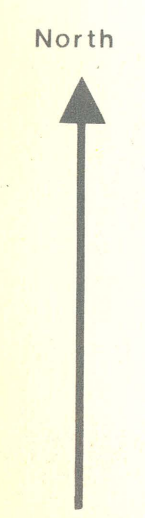
64° 45' N

64° 45' N

LEGEND

Gabbro – Quartz Gabbro Dyke ☆
where 1 : Quartz Gabbro phase
2 : Gabbro phase

Quartz Monzodiorite

Granite

Coarse marginal Granite phase

Hornblende Quartz Syenite

Rhyolite

Andesite Tuff

☆ where lighter shades represent exrapolation between outcrops

⎯⎯ known contact
– – – assumed contact
· · · outcrop boundary
⎯·⎯· assumed compositional boundary within unit

╱ clast orientation
○ sample
● sample – thin section
★ sample – chemistry

Geology of an Area of Igneous Intrusives: Southwest corner.

Back River Volcanic Complex, District of Mackenzie.

Northwest Territories

Coronation
Gulf
●map
Gt.
Slave
Lake

SCALE:

30·5 m.
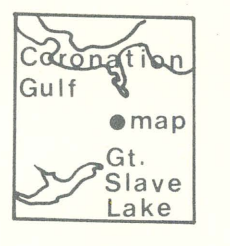
Geology by D. L. Beaumont – June 1977

108° 00' W